Table 3a
Genes induced by exemestane treatment in hFOB cells—2.0 higher

	Gene title	Gene symbol	Raw data			Ratio	
			C	D	Ex	D	Ex
NM_002466	V-myb myeloblastosis viral oncogene homolog (avian)-like 2	**MYBL2**	70.9	156.9	150.3	2.2	2.1
AW444985	–	–	57.8	124.7	127.1	2.2	2.2
AF143684	Myosin IXB	MYO9B	48.3	64.4	122.2	1.3	2.5
NM_024682	TBC1 domain family, member 17	TBC1D17	31.7	37.6	64.8	1.2	2.0
BE965311	Chromosome 16 open reading frame 23	C16orf23	29.2	44.2	64.0	1.5	2.2
NM_004233	CD83 antigen (activated B lymphocytes, immunoglobulin superfamily)	CD83	29.0	66.5	60.9	2.3	2.1
AI806031	Skeletal muscle and kidney enriched inositol phosphatase	SKIP	27.7	48.6	55.4	1.8	2.0
AL136729	Ring finger protein 123	RNF123	20.0	23.7	41.3	1.2	2.1
NM_015254	Kinesin family member 13B	KIF13B	13.0	24.5	39.4	1.9	3.0
AL110249	Chromosome 20 open reading frame 194	C20orf194	13.4	39.0	29.7	2.9	2.2
AF208502	Early B-cell factor	EBF	12.5	21.1	28.5	1.7	2.3
AW007221	Solute carrier family 13 (sodium/sulfate symporters), member 4	SLC13A4	12.3	9.6	27.8	0.8	2.3
AB007458	TP53 activated protein 1	TP53AP1	12.6	22.2	26.2	1.8	2.1
AV713913	Osteopetrosis associated transmembrane protein 1	**OSTM1**	9.8	16.5	21.3	1.7	2.2
BF339201	THAP domain containing 6	THAP6	6.0	14.0	20.6	2.3	3.4
AK000455	Hypothetical gene MGC16733 similar to CG12113	MGC16733	7.3	16.6	18.8	2.3	2.6
AW974816	–	–	2.2	16.0	17.2	7.2	7.7
AK025325	Transcribed locus, moderately similar to NP_689573.2 zinc finger protein 573	–	7.3	11.4	16.2	1.6	2.2
NM_021192	Homeo box D11	**HOXD11**	5.3	16.2	15.8	3.0	3.0
NM_022169	ATP-binding cassette, sub-family G (WHITE), member 4	ABCG4	7.0	10.5	15.7	1.5	2.2
R62907	Disabled homolog 2, mitogen-responsive phosphoprotein (*Drosophila*)	DAB2	7.7	13.0	15.5	1.7	2.0
NM_002661	Phospholipase C, gamma 2 (phosphatidylinositol-specific)	PLCG2	7.3	12.3	15.3	1.7	2.1
BG393032	Solute carrier family 13 (sodium/sulfate symporters), member 4	SLC13A4	6.4	6.7	15.1	1.0	2.3
BC002794	Tumor necrosis factor receptor superfamily, member 14	TNFRSF14	6.2	11.3	13.6	1.8	2.2
BC042908	KIAA0690	KIAA0690	5.6	7.4	13.5	1.3	2.4
AW451961	Adenylate cyclase activating polypeptide 1 (pituitary) receptor type I	**ADCYAP1R1**	4.3	11.7	13.2	2.7	3.1
AI863264	Glypican 2 (cerebroglycan)	**GPC2**	5.3	7.2	13.2	1.3	2.5
AF130050	ACA47 scaRNA gene	-	5.6	9.5	12.9	1.7	2.3
AK022326	Hypothetical gene supported by AK022326	-	6.1	12.7	12.9	2.1	2.1
AK021807	Low density lipoprotein receptor-related protein 11	LRP11	5.9	6.2	12.8	1.0	2.2
AU155415	Kallikrein 7 (chymotryptic, stratum corneum)	KLK7	5.6	13.5	12.7	2.4	2.3
BF673779	Hypothetical protein FLJ30834	FLJ30834	5.5	6.3	12.3	1.1	2.2
AV646335	–	–	2.6	13.0	11.2	5.0	4.3
BC040600	–	–	5.0	5.4	10.6	1.1	2.1
AI131035	–	–	5.1	9.2	10.5	1.8	2.1

C, vehicle control; D, 5α-dihydrotestosterone; Ex, exemestane. Genes that performed quantitative RT-PCR were described in bold style.

Microarray/clustering analysis

In hFOB cells, the hierarchical clustering analysis contains 430 genes which demonstrated expression ratios above 2.0-fold and below 0.5-fold compared with vehicle control cells after 12 h of each gene treated with 10^{-8} M E2, 10^{-8} M DHT, or 10^{-7} M EXE. The expression profiles of EXE treated cells were closely related to those of DHT (Fig. 5). In this study, we focused on 35 genes (Table 3a), which were all up-regulated twice or more than control. In this group, we further focused on 5 genes, B-Myb 2 (MYBL2), osteopetrosis associated transmembrane protein 1 (OSTM1), homeo box D 11 (HOXD11), adenylate cyclase activating polypeptide 1 receptor (ADCYAP1R1), and glypican 2 (GPC2) which are all considered to play important roles in EXE or DHT induced cell proliferation. We therefore examined whether these 5 genes were increased by EXE or DHT treatments using quantitative RT-PCR in hFOB cells. We also examined the validation of results of microarray analysis obtained in hFOB cells in Saos-2 and MG-63 cells.

Validation of microarray analysis using quantitative RT-PCR

In hFOB cells, all of these 5 genes described above were significantly increased by 10^{-7} M EXE treatment, and 3/5 genes (except for OSTM1 and GPC2) were also significantly increased by 10^{-8} M DHT treatment. HOXD11 and ADCYAP1R1 genes increased by both EXE and DHT were significantly diminished by OHF (5×10^{-6} M) treatment (Figs. 6A–C).

The similar results of changes of MYBL2 expression were also obtained in both Saos-2 and MG-63 treated with EXE and DHT, respectively (Fig. 6A). In addition, the results of HOXD11 expression in hFOB were equivalent to those in Saos-2 but not in MG-63 treated with EXE and DHT (Fig. 6B). Other genes induced by treatment of EXE and DHT in hFOB such as OSTM1, GPC2, and ADCYAP1R1 were not changed in both Saos-2 and MG-63 cells treated with EXE and DHT, respectively (data not present). AI-I or AGM treatment did not increase all of these genes expression in hFOB (data not present).

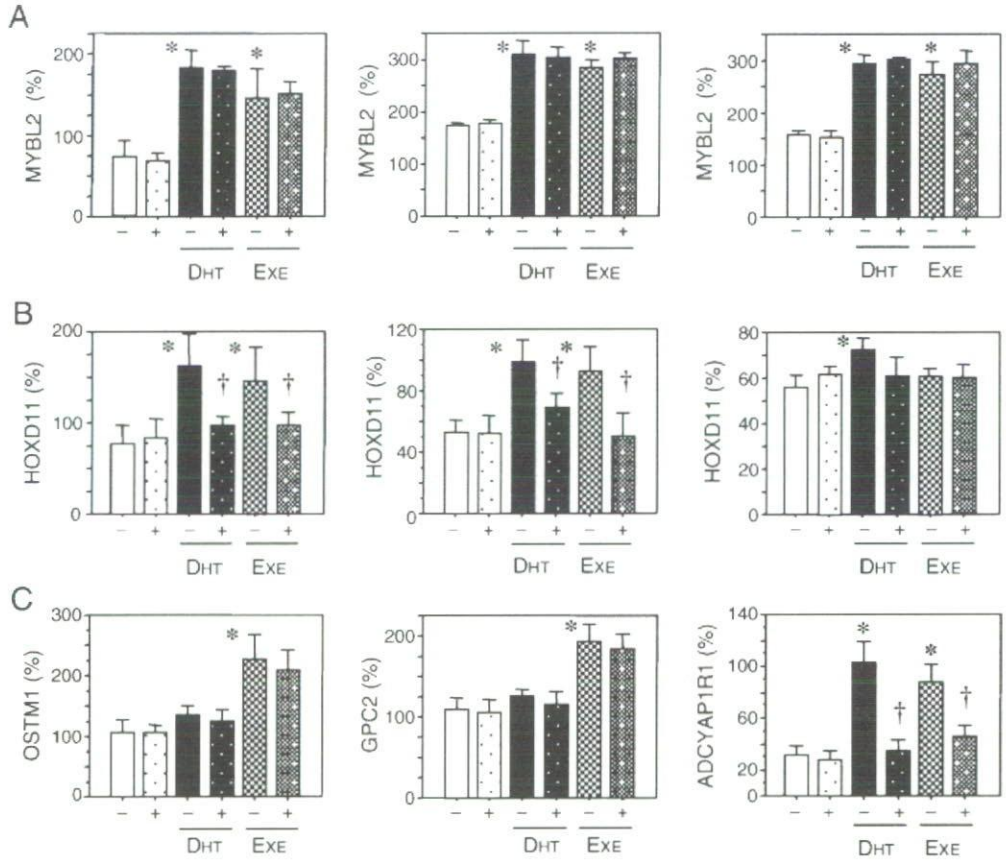

Fig. 6. Validation of microarray analysis. (A) Expression levels of MYBL2 in hFOB (left), Saos-2 (middle), and MG-63 (right). (B) Expression levels of HOXD11 in hFOB (left), Saos-2 (middle), and MG-63 (right). (C) Expression levels of OSTM1, GPC2, and ADCYAP1R1 in hFOB. DHT: 10^{-8} M 5α-dihydrotestosterone, EXE: 10^{-7} M Exemestane, with (+) or without (−) hydroxyflutamide, $p<0.05$ vs. control (*) or without hydroxyflutamide (†).

Analysis of osteoblast growth-related genes

Results of microarray analysis in hFOB cell demonstrated that osteoblast growth-related genes [24,25] such as COL1A1, SMAD1, SMAD5, SPARC, and RUNX2 were all up-regulated by exemestane (10^{-7} M) treatment but the degrees of increment were all under 2-fold (Table 3b). In this microarray analysis, other expression levels of previously reported osteoblast-related genes were not altered.

In hFOB cells, the validation analysis of these genes described above using quantitative RT-PCR (Fig. 7) demonstrated that 4/5 genes (except for COL1A1) were significantly increased by 10^{-7} M EXE treatment, and 4/5 genes (except for SMAD1) were also significantly increased by 10^{-8} M DHT treatment. The increased expression of the SMAD1, SMAD5, and SPARC genes by EXE or DHT, was significantly diminished by OHF (5×10^{-6} M) treatment. There were no effects of OHF pretreatment on the increased expression levels of RUNX2 that had occurred after both EXE and DHT treatments. Both AI-I and AGM treatment could not increase all of these genes expression in hFOB (data not present).

In Saos-2 cells, 4/5 genes (except for RUNX2) were significantly increased by 10^{-7} M EXE treatment, and 3/5 genes (except for RUNX2 and SMAD1) were also significantly increased by 10^{-8} M DHT treatment. The increment of the COL1A1, SMAD5, and SPARC genes expression by EXE or DHT, was significantly diminished by OHF (5×10^{-6} M) treatment. All of these 5 genes did not change in MG-63 cells treated with EXE or DHT, respectively (data not present).

Immunohistochemistry of AR

Marked AR immunoreactivity was detected in the nuclei of osteoblasts or lining cells but not in osteoclasts in four cases (Fig. 8). In these four cases, AR immunoreactivity was also detected in osteocytes and condrocytes. In one case, there was no immunoreactivity in all types of bone cells.

Discussion

In the clinical study of EXE compared to placebo administrated for two years [26,27], EXE modestly enhanced bone loss from the femoral neck without significant influence on lumber bone loss despite a marked systemic estrogen depletion. Furthermore, the risks of clinical bone fractures are considered to be lower with EXE treatment than that seen with non steroidal AIs [27,28], though it is also important to recognize that EXE has not been shown to significantly increase the amount of bone mass in various clinical studies of breast cancer patients [26,27]. The relative protective effect of EXE, a

Table 3b
Genes induced by exemestane treatment in hFOB cells—the osteoblast growth-related genes

	Gene title	Gene symbol	Raw data			Ratio	
			C	D	Ex	D	Ex
K01228	Collagen, type I, alpha 1	**COL1A1**	2797.2	3240.9	3058.5	1.2	1.1
BE221212	Collagen, type I, alpha 1	**COL1A1**	2741.1	3048.3	3052.2	1.1	1.1
AI743621	Collagen, type I, alpha 1	**COL1A1**	228.0	241.6	242.5	1.1	1.1
AA788711	Collagen, type I, alpha 2	COL1A2	2250.6	2474.3	2375.4	1.1	1.1
NM_000089	Collagen, type I, alpha 2	COL1A2	1749.1	1848.7	1787.6	1.1	1.0
M60485	Fibroblast growth factor receptor 1	FGFR1	178.9	185.7	198.6	1.0	1.1
BE467261	Fibroblast growth factor receptor 1	FGFR1	165.4	208.6	189.7	1.3	1.1
M63889	Fibroblast growth factor receptor 1	FGFR1	119.3	111.6	140.5	0.9	1.2
NM_023110	Fibroblast growth factor receptor 1	FGFR1	60.5	84.0	70.2	1.4	1.2
AU145411	Fibroblast growth factor receptor 1	FGFR1	29.2	44.1	37.5	1.5	1.3
AI359368	Fibroblast growth factor receptor 3	FGFR3	41.4	65.5	58.7	1.6	1.4
NM_001552	Insulin-like growth factor binding protein 4	IGFBP4	809.1	1027.5	1040.4	1.3	1.3
AL353944	Runt-related transcription factor 2	**RUNX2**	192.9	226.3	216.3	1.2	1.1
AU146891	SMAD, mothers against DPP homolog 1 (*Drosophila*)	**SMAD1**	161.2	195.6	204.6	1.2	1.3
NM_005901	SMAD, mothers against DPP homolog 2 (*Drosophila*)	SMAD2	100.3	108.2	113.7	1.1	1.1
NM_005902	SMAD, mothers against DPP homolog 3 (*Drosophila*)	SMAD3	110.2	106.5	127.7	1.0	1.2
BF526175	SMAD, mothers against DPP homolog 5 (*Drosophila*)	**SMAD5**	361.0	488.3	514.2	1.4	1.4
AI478523	SMAD, mothers against DPP homolog 5 (*Drosophila*)	SMAD5	300.7	384.9	346.9	1.3	1.2
AF010601	SMAD, mothers against DPP homolog 5 (*Drosophila*)	SMAD5	79.2	99.7	87.6	1.3	1.1
AY014180	SMAD-specific E3 ubiquitin protein ligase 2	SMURF2	804.2	844.7	851.8	1.1	1.1
AU157259	SMAD-specific E3 ubiquitin protein ligase 2	SMURF2	77.1	81.5	86.3	1.1	1.1
AL575922	Secreted protein, acidic, cysteine-rich (osteonectin)	**SPARC**	1702.1	1935.5	1925.8	1.1	1.1
BF508662	Sprouty homolog 1, antagonist of FGF signaling (*Drosophila*)	SPRY1	31.9	46.3	45.4	1.5	1.4
NM_014886	TGF beta-inducible nuclear protein 1	TINP1	1185.7	1259.5	1241.1	1.1	1.0

C, vehicle control; D, 5α-dihydrotestosterone; Ex, exemestane. Genes that performed quantitative RT-PCR were described in bold style.

steroidal aromatase inhibitor, has been therefore attributed to its actions through AR in osteoblasts. Systemic androgenic effects such as hypertricosis, hair loss, hoarseness, and acne have been reported only in 4% [6] of the patients treated with EXE (25 mg/day) and the frequency of these effects increases to approximately 10% in those treated with higher dose 200 mg/day of EXE [6]. This finding suggests that the patients treated with EXE are under relatively weak systemic androgenic effects. Androgen sensitivity has been well-known to be subject to great individual variation caused by AR gene CAG polymorphism in women as well as men [29,30]. Therefore, this 5 to 10% of the patients who manifested clinical androgenic effects by EXE treatment may be individuals associated with relatively enhanced androgenic sensitivity. Replacement therapy with TST is generally effective at restoring bone in hypogonadal men [31]. In female-to-male, genetic female transsexual subjects, high-dose TST therapy generally increased BMD at the femoral neck, despite decrement of E2 to postmenopausal levels [32,33]. Therefore, androgens may play an important role in bone protection in women as well as men.

The results of cell proliferation assay demonstrated that the cell number of MG-63 was increased by both E2 and DHT treatments, but the dose of DHT was relatively higher than that in two other cells. MG-63 expressed higher levels of ERα/β mRNA, but the level of AR mRNA was lower than that in both Saos-2 and hFOB. Both cell proliferation and ALP activity of MG-63 could not be stimulated by EXE treatment. Molecular mechanisms of androgen actions on osteoblasts have remained largely unknown. Androgen is well-known to stimulate osteoblast proliferation [34] and differentiation [35]. For instance, osteoprotegerin mRNA was increased by TST as well as DHT treatments in mouse 3T3-E1 cells [36].

AR and ERβ but not ERα are predominantly detected in osteoblasts located on human cancellous bone using immunohistochemical analysis [37]. Therefore, hFOB examined in this study is considered to maintain relatively native status of sex steroids pathways in human osteoblasts. Therefore, we employed hFOB for further examination of EXE effects on osteoblast gene expression pattern using microarray analysis. In this study, we demonstrated that the genes MYBL2 [38], OSTM1 [39], HOXD11 [40], ADCYAP1R1 [41], and GPC2 [42] were target genes of EXE alone or both EXE and DHT in hFOB using microarray/PCR analysis. These genes were demonstrated to be involved in regulation of cell cycle, differentiation, and transcription. In EXE or DHT treatment in hFOB and Saos-2, in which cells proliferations were stimulated, an increased expression of HOXD11 gene was detected. The product of the mouse Hoxd11 gene was reported to play a role in forelimb morphogenesis [40,43]. Therefore, these finding suggest that osteoblast cell proliferation stimulated by EXE treatment may depend on HOXD11 gene expression through AR. In this study, the cell proliferation of MG-63, which expressed relatively low level of AR, was not stimulated by EXE. In addition, HOXD11 gene expression was not up-regulated by EXE treatment in MG-63 cells. These results were also consist with the protective effects of EXE through potential androgen-HOXD11 pathway in osteoblast cells. In this study, we also examined the effects of EXE and DHT on osteoblast growth-related genes using micro-

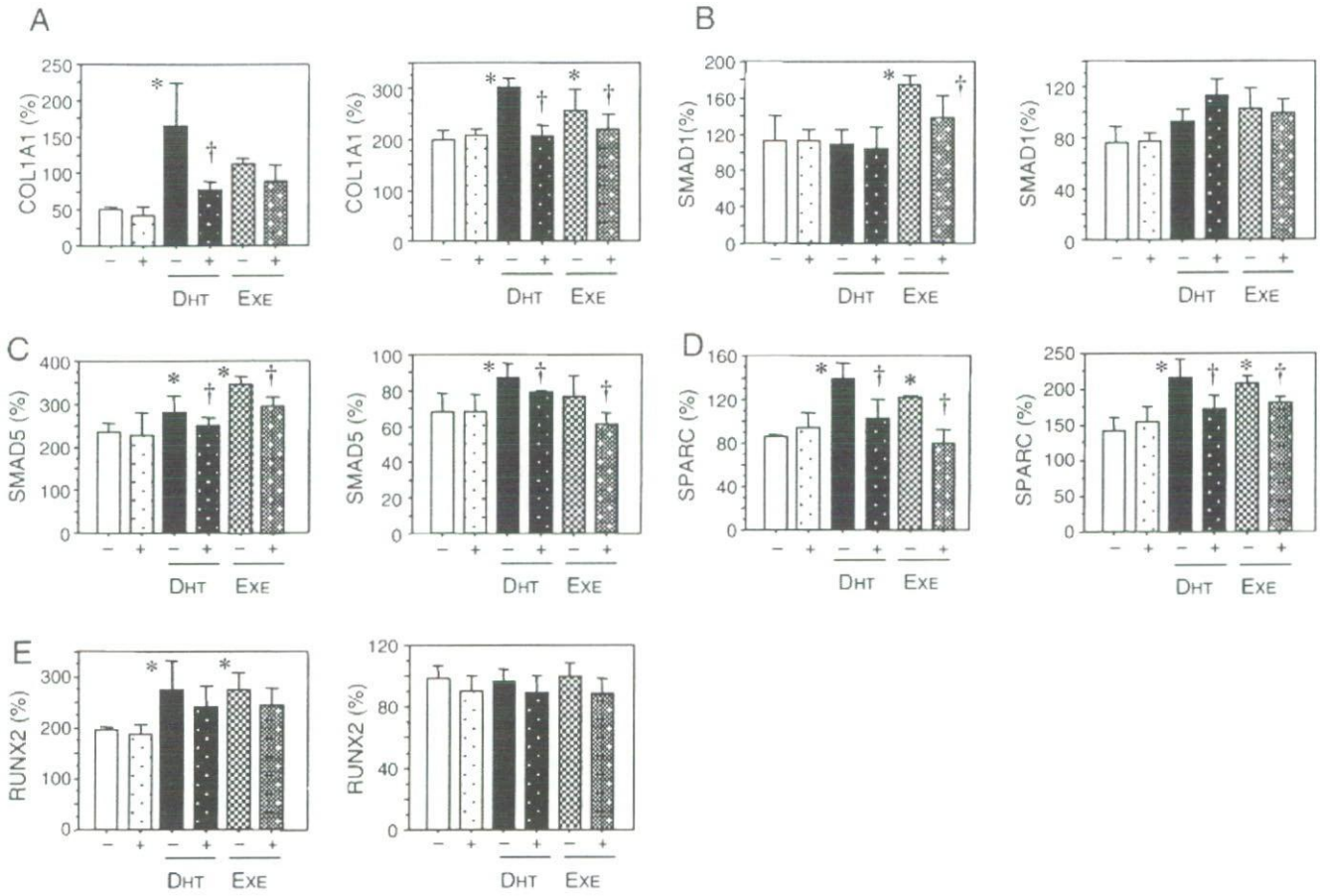

Fig. 7. Expression levels of osteoblast growth-related genes in hFOB (left) and Saos-2 (right). DHT: 10^{-8} M 5α-dihydrotestosterone, EXE: 10^{-7} M Exemestane, with (+) or without (−) hydroxyflutamide, $p<0.05$ vs. control (*) or without hydroxyflutamide (†).

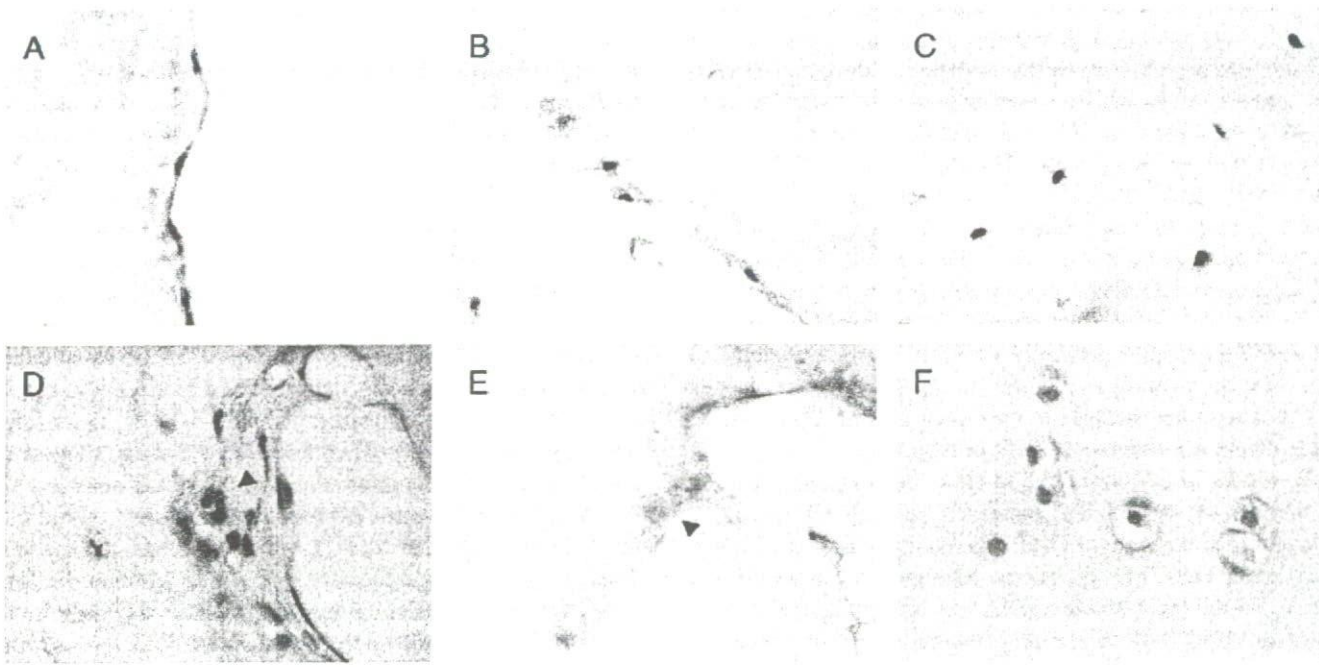

Fig. 8. Immunohistochemistry of androgen receptor in human bone tissues. Immunoreactivity of androgen receptor was detected in nuclei of osteoblasts/liner cells (A, B) but not in osteoclasts (D, E; arrowheads). Immunoreactivity of androgen receptor was also detected in nuclei of osteocytes (C) and condrocytes (F).

array analysis and following quantitative RT-PCR. COL1A1, SMAD5, and SPARC (osteonectine) were up-regulated by EXE and/or DHT treatments in both hFOB and Saos-2 cells. EXE or DHT treatments in both hFOB and Saos-2 also resulted in increased ALP activity. There have been, however, no studies reported on whether these genes are primary or secondary androgen responsive genes in osteoblasts. The AR-specific antagonist, OHF demonstrated no inhibitory effects on RUNX2 expression increased by EXE or DHT treatment in hFOB cells. In addition, hFOB cell growth induced by high dose of EXE treatment was not completely inhibited by OHF treatment. These results all suggest that EXE also may stimulate hFOB cell proliferation through both AR dependent and independent pathways. From our data of steroid production in hFOB, EXE may have an additional androgenic effect through increased TST levels in conjunction with inhibition of aromatization in hFOB cells. However, it awaits further investigations for clarification.

In normal bone remodeling, bone formation by osteoblasts follows bone resorption by osteoclasts and occurs in a precise and quantitative manner (coupling). In this coupling between bone formation and resorption, a coupling factor that induces bone formation is considered to be released during osteoclastic bone resorption [44]. This study has focused on the specific effects on osteoblast cells. However, it is true that there were significant increases in both serum bone formation and resorption markers in postmenopausal women administered with EXE for 2 years [26]. Osteoclasts, which are responsible for bone resorption, are target cells for many anti-osteoporosis therapeutic agents such as bisphosphonate of postmenopausal women [45]. However, it is unclear whether EXE acts on osteoclast directly. Chen et al. [46] reported that testosterone inhibited osteoclast formation stimulated by parathyroid hormone through the AR but not through the production of intrinsic estrogen using primary mouse osteoclast cells. In both human and rodent bone tissues, AR is expressed in both osteoblasts and osteocytes [47,48]. However, AR is detected in osteoclasts of rodent but not in human cells [31,47,48]. Therefore, in humans, androgens are considered to exert their effects on bone through osteoblasts. EXE may therefore exert its possible androgenic effects on human bone through osteoblasts but not osteoclasts. Results of our present study also suggest the possible roles of EXE on osteoblast cells through AR independent manner. Results of clinical studies suggest that the combination therapy of AI and COX-2 inhibitors could provide more effective aromatase inhibition than single therapy in hormone-sensitive postmenopausal breast cancer [49]. Bone resorption induced by IL-1 and IL-6 was also reported to occur via stimulation of COX-2 dependent PGE_2 production in osteoblasts *in vitro* [50]. Therefore, further investigations are required to clarify the effects of AI including EXE on human bone tissues.

In summary, this study using osteoblast and osteoblast-like cell lines suggested the potential protective effect of steroidal AI, EXE on osteoblasts occurred through both AR dependent and independent pathways. HOXD11 gene known as bone morphogenesis factor and osteoblast growth-related genes were induced by EXE treatment as well as DHT treatment in both hFOB and Saos-2. Damages of bone tissues by estrogen depletion caused by AI administration are considered unavoidable but the selection of potential hormone therapies which could minimize the damages or injuries of bone tissues is considered important.

Acknowledgments

We appreciate Dr. Shin-ichi Hayashi (Divisions of Molecular Medical Technology, Tohoku University School of Medicine) for critical comments. We also appreciate Ms. Chika Tazawa, Ms. Toshie Suzuki, Ms. Miki Mori and Mr. Katsuhiko Ono (Department of Pathology, Tohoku University School of Medicine) for skillful technical assistances. This research was supported by Grant-in-aid for Health and Labor Sciences Research Grant on Risk of Chemical Substances (H16-Kagaku-002) from Ministry of Health, Labor, and Welfare, Japan and Kanzawa Medical Research Foundation, Nagano, Japan.

References

[1] Rogers J. Estrogens in the menopause and postmenopause. N Engl J Med 1969;280:364–7.
[2] Wingate L. The epidemiology of osteoporosis. J Med 1984;15:245–66.
[3] Felson DT, Zhang Y, Hannan MT, Kiel DP, Wilson PW, Anderson JJ. The effect of postmenopausal estrogen therapy on bone density in elderly women. N Engl J Med 1993;329:1141–6.
[4] Lester L, Coleman R. Bone loss and the aromatase inhibitors. Br J Cancer 2005;93:S16–22.
[5] Miller WR, Dixon JM. Antiaromatase agents: preclinical data and neoadjuvant therapy. Clin Breast Cancer 2000;1:S9–S14.
[6] Lønning PE, Paridaens R, Thurlimann B, Piscitelli G, di Salle E. Exemestane experience in breast cancer treatment. J Steroid Biochem Mol Biol 1997;61:151–5.
[7] Center for Drug Evaluation and Research Application Number NDA 20753 (Exemestane) Medical Review. Food and Drug Administration, 1999.
[8] Goss PE, Qi S, Josse RG, Pritzker KPH, Mendes M, Hu H, et al. The steroidal Aromatase inhibitor exemestane prevent bone loss in ovariectomized rats. Bone 2004;34:384–92.
[9] Goss PE, Qi S, Cheung AM, Hu H, Mendes M, Pritzker KPH. Effects of steroidal aromatase inhibitor exemestane and the nonsteroidal aromatase inhibitor letrozole on bone and lipid metabolism in the ovariectomized rats. Clin Cancer Res 2004;10:5717–23.
[10] Sasano H, Uzuki M, Sawai T, Nagura H, Matsunaga G, Kashimoto O, et al. Aromatase in human bone tissue. J Bone Miner Res 1997;12:1416–23.
[11] Schweikert HU, Wolf L, Romalo G. Oestrogen formation from Androstendione in human bone. Clin Endocrinol 1995;43:37–42.
[12] Purohit A, Flanagan AM, Reed MJ. Estrogen synthesis by osteoblast cell lines. Endocrinology 1992;131:2027–9.
[13] Tanaka S, Haji M, Nishi Y, Yanase T, Takayanagi R, Nawata H. Aromatase activity in human osteoblast-like osteosarcoma cell. Calcif Tissue Int 1993;52:107–9.
[14] Recanatini M, Bisi A, Cavalli A, Belluti F, Gobbi S, Rampa A, et al. A new class of nonsteroidal aromatase inhibitors: design and synthesis of chromone and xanthone derivatives and inhibition of the P450 enzymes aromatase and 17 alpha-hydroxylase/C17,20-lyase. J Med Chem 2001;44:672–80.
[15] Linkhart TA, Mohan S, Baylink DJ. Growth factors for bone growth and repair: IGF, TGF beta and BMP. Bone 1996;19:1S–12S.
[16] Harris SA, Enger RJ, Riggs BL, Spelsberg TC. Development and characterization of a conditionally immortalized human fetal osteoblastic cell line. J Bone Miner Res 1995;10:178–86.
[17] Suzuki T, Darnel AD, Akahira JI, Ariga N, Ogawa S, Kaneko C, et al. 5alpha-reductases in human breast carcinoma: possible modulator of in situ androgenic actions. J Clin Endocrinol Metab 2001;86:2250–7.

[18] Miki Y, Suzuki T, Tazawa C, Ishizuka M, Semba S, Gorai I, et al. Analysis of gene expression induced by diethylstilbestrol (DES) in human primitive Müllerian duct cells using microarray. Cancer Lett 2005;220:197–210.
[19] Yamamoto M, Takahashi Y, Tabata Y. Controlled release by biodegradable hydrogels enhances the ectopic bone formation of bone morphogenetic protein. Biomaterials 2003;24:4375–83.
[20] Kanno J, Aisaki K, Igarashi K, Nakatsu N, Ono A, Kodama Y, et al. "Per cell" normalization method for mRNA measurement by quantitative PCR and microarrays. BMC Genomics 2006;29:64.
[21] Eisen MB, Spellman PT, Brown PO, Bostein D. Cluster analysis and display of genome-wide expression patterns. Proc Natl Acad Sci U S A 1998;95:14863–8.
[22] Miki Y, Nakata T, Suzuki T, Darnel AD, Moriya T, Kaneko C, et al. Systemic distribution of steroid sulfatase and estrogen sulfotransferase in human adult and fetal tissues. J Clin Endcrinol Metab 2002;87:5760–8.
[23] Ishizuka M, Hatori M, Suzuki T, Miki Y, Darnel AD, Tazawa C, et al. Sex steroid receptors in rheumatoid arthritis. Clin Sci (Lond) 2004;106: 293–300.
[24] Rodan GA, Noda M. Gene expression in osteoblastic cells. Crit Rev Eukaryot Gene Expr 1991;1:85–98.
[25] Ito Y, Miyazono K. RUNX transcription factors as key role of TGF-β superfamily signaling. Curr Opin Genet Dev 2003;13:43–7.
[26] Lønning PE, Geisler J, Krag LE, Erikstein B, Bremnes Y, Hagen AI, et al. Effects of exemestane administered for 2 years versus placebo on bone mineral density, bone biomarkers, and plasma lipids in patients with surgically respected early breast cancer. J Clin Oncol 2005;23:4847–9.
[27] Coombes RC, Hall E, Gibson LJ, Paridaens R, Jassem J, Delozier T, et al. Intergroup Exemestane Study. A randomized trial of exemestane after two to three years of tamoxifen therapy in postmenopausal women with primary breast cancer. N Engl J Med 2004;350:1081–92.
[28] Coleman RE, Banks LM, Girgis SI, Vrdoljak E, Fox J, Porter LS, et al. Skeletal effect of exemestane in the Intergroup Exemestane Study (IES)—2 years bone mineral density (BMD) and bone biomarker data. Breast Cancer Res Treat 2005;94:S233.
[29] Vottero A, Stratalis CA, Ghizzoni L, Longui CA, Karl M, Chrousos GP. Androgen receptor-mediated hypersensitivity to androgen in women with nonhyperandrogenic hirsutism: skewing of X-chromosome inactivation. J Clin Endocrinol Metab 1999;84:1091–5.
[30] Brum IS, Spritzer PM, Paris F, Maturana MA, Audran F, Sultan C. Association between androgen receptor gene CAG repeat polymorphism and plasma testosterone levels in postmenopausal women. J Soc Gynecol Investig 2005;12:135–41.
[31] Vanderschueren D, Vandenput L, Boonen S, Lindberg MK, Bouillon R, Ohlsson C. Androgens and bone. Endocr Rev 2004;25:389–425.
[32] Turner A, Chen T, Barber T, Malabanan A, Holick M, Tangpricha V. Testosterone increases bone mineral density in female-to-male transsexuals: a case series of 15 subjects. Clin Endocrinol (Oxf) 2004;61:560–6.
[33] Ruetsche AG, Kneubuehl R, Birkhaeuser MH, Lippuner K. Cortical and trabecular bone mineral density in transsexuals after long-term cross-sex hormonal treatment: a cross-sectional study. Osteoporos Int 2005;16: 791–98.
[34] Kasperk CH, Wergedal JE, Farley JR, Linkhart TA, Turner RT, Baylink DJ. Androgens directly stimulate proliferation of bone cells in vitro. Endocrinology 1989;124:1576–8.
[35] Kasperk C, Fitzsimmons R, Strong D, Mohan S, Jennings J, Wergedal J, et al. Studies of the mechanism by which androgens enhance mitogenesis and differentiation in bone cells. J Clin Endocrinol Metab 1990;71:1322–9.
[36] Chen Q, Kaji H, Kanatani M, Sugimoto T, Chihara K. Testosterone increases osteoprotegerin mRNA expression in mouse osteoblast cells. Horm Metab Res 2004;36:674–8.
[37] Bord S, Horner A, Beavan S, Compston J. Estrogen receptors alpha and beta are differentially expressed in developing human bone. J Clin Endocrinol Metab 2001;86:2309–14.
[38] Sala A, Watson R. B-Myb protein in cellular proliferation, transcription control, and cancer: latest developments. J Cell Physiol 1999;179:245–50.
[39] Chalhoub N, Benachenhou N, Rajapurohitam V, Pata M, Ferron M, Frattini A, et al. Grey-lethal mutation induces severe malignant autosomal recessive osteopetrosis in mouse and human. Nat Med 2003;9:399–406.
[40] Boulet AM, Capecchi MR. Multiple roles of Hoxa11 and Hoxd11 in the formation of the mammalian forelimb zeugopod. Development 2004; 131:299–309.
[41] Lundberg P, Lundgren I, Mukohyama H, Lehenkari PP, Horton MA, Lerner UH. Vasoactive intestinal peptide (VIP)/pituitary adenylate cyclase-activating peptide receptor subtypes in mouse calvarial osteoblasts: presence of VIP-2 receptors and differentiation-induced expression of VIP-1 receptors. Endocrinology 2001;142:339–47.
[42] Gutierrez J, Osses N, Brandan E. Changes in secreted and cell associated proteoglycan synthesis during conversion of myoblasts to osteoblasts in response to bone morphogenetic protein-2: role of decorin in cell response to BMP-2. J Cell Physiol 2006;206:58–67.
[43] Omi M, Fisher M, Maihle NJ, Dealy CN. Studies on epidermal growth factor receptor signaling in vertebrate limb patterning. Dev Dyn 2005;233:288–300.
[44] Rodan GA, Raisz LG, Bilezikian JP. Pathophysiology of osteoporosis. . (chapter 73)In: Bilezikian JP, Raisz LG, Rodan GA, editors. Principles of bone biology, 2nd ed., vol. 1. NY, USA: Academic Press, A division of Harcourt, Inc.; 2002. p. 1275–90.
[45] Kellinsalmi M, Monkkonen H, Monkkonen J, Leskela HV, Parikka V, Hamalainen M, et al. In vitro comparison of clodronate, pamidronate and zoledronic acid effects on rat osteoclasts and human stem cell-derived osteoblasts. Basic Clin Pharmacol Toxicol 2005;97:382–91.
[46] Chen Q, Kaji H, Sugimoto T, Chihara K. Testosterone inhibits osteoclast formation stimulated by parathyroid hormone through androgen receptor. FEBS Lett 2001;491:91–3.
[47] Abu EO, Horner A, Kusec V, Triffitt JT, Compston JE. The localization of androgen receptors in human bone. J Clin Endocrinol Metab 1997; 82:3493–7.
[48] Wiren KM, Orwoll ES. Androgens: receptor expression and steroid action in bone. . (chapter 43)In: Bilezikian JP, Raisz LG, Rodan GA, editors. Principles of bone biology, 2nd ed., vol. 1. NY, USA: Academic Press, A division of Harcourt, Inc.; 2002. p. 757–72.
[49] Chow LW, Wong JL, Toi M. Celecoxib anti-aromatase neoadjuvant (CAAN) trial for locally advanced breast cancer: preliminary report. J Steroid Biochem Mol Biol 2003;86:443–7.
[50] Sato T, Morita I, Sakaguchi K, Nakahama KI, Smith WL, Dewitt DL, et al. Involvement of prostaglandin endoperoxide H synthase-2 in osteoclast-like cell formation induced by interleukin-1 beta. J Bone Miner Res 1996;11:392–400.

Available online at www.sciencedirect.com
ScienceDirect
Biomedicine & Pharmacotherapy 61 (2007) 540–542
BIOMEDICINE & PHARMACOTHERAPY
www.elsevier.com/locate/biopha

Aromatase inhibitor and bone

Yasuhiro Miki, Takashi Suzuki, Hironobu Sasano*

Department of Pathology, Tohoku University Graduate School of Medicine, 2-1 Seiryo-machi, Aoba-ku, Sendai, Miyagi 980 8575, Japan

Available online 14 September 2007

Abstract

Aromatase is a key enzyme of intratumoral production of estrogen in breast cancers. Aromatase inhibitors are commonly used as hormone therapy in postmenopausal estrogen sensitive breast cancer patients. Type I aromatase inhibitors such as exemestane are steroidal inhibitors, which have androstenedione like structure and bind to androgen receptor with low affinity. Type II aromatase inhibitors such as anastrozole and letrozole are known as non-steroidal inhibitors, which are non-competitive inhibitors of aromatase. Sex steroid hormones such as estrogen and androgen play important roles in the maintenances of female and male bone tissues. It is well known that adult women have less bone mass than men. Especially after menopause, adult women loss their bone mass more rapidly than men of comparable age do. Therefore, many clinical reports of breast cancer patients treated with aromatase inhibitors have emphasized potential bone loss caused by aromatase inhibition. Several basic researches using animal model or *in vitro* model demonstrated the different effects of steroid and non-steroid aromatase inhibitors on bone tissues and cells. In this review, we summarize the effects of AIs on bone tissues reported in clinical studies and animal/*in vitro* studies.

Keywords: Aromatase inhibitor; Bone; Osteoblast

1. Introduction

Estrogens play important roles in the development of hormone-dependent breast carcinomas. The postmenopausal women have low levels of circulating estrogens, however, local synthesis of estrogens takes place in breast tissue [1,2]. Local production of estrogens in human breast carcinoma tissues through aromatization caused by cytochrome P450 19 (aromatase) of androgens into estrogens has been demonstrated [3]. Intratumoral aromatase has been established as the important target of the breast cancer endocrine therapy in hormone-dependent postmenopausal patients. Two types of aromatase inhibitor (AI) currently available (Table 1) have different mechanisms of actions. Agents that interfere with the substrate-binding sites of the enzyme are androgen analogues known as steroidal AI (type 1 AI; e.g., exemestane, formestane) [4]. Agents that block the electron transfer chain by the cytochrome P450 prosthetic group of aromatase are known as non-steroidal AI (type II AI; e.g., letrozole, anastrozole, aminoglutethimide) [4].

It is well known that sex steroid hormones such as estrogen and androgen play an important role in the maintenance of bone tissues [5]. The reductions in circulating estrogen levels that occur at the menopause are related with a rapid deterioration in bone density by as much as 3% per year for the first 5 years following the menopause [6]. Therefore, several bone damage such as osteoporosis and fracture have been reported to arise along with further estrogen depletion caused by AI treatment in postmenopausal breast cancer patients.

2. AIs and bone: clinical studies

Several clinical trials in postmenopausal breast cancer patients treated with aromatase inhibitors evaluated the risks of bone fractures. In ATAC [Arimidex (anastrozole) and Tamoxifen Alone or in Combination] trial at a median follow-up of 68 months, an increase in clinical bone fracture occurred in the patients treated with anastrozole despite greater clinical efficacy of anastrozole over tamoxifen [7]. Similar results were also reported in BIG (Breast International Group) 1-98 trial

* Corresponding author. Tel.: +81 22 717 7450; fax: +81 22 273 5976.
E-mail address: hsasano@patholo2.med.tohoku.ac.jp (H. Sasano).

0753-3322/$ - see front matter © 2007 Elsevier Masson SAS. All rights reserved.
doi:10.1016/j.biopha.2007.08.011

Table 1
Aromatase inhibitors by generation and type

Generation	Type 1 (steroidal inhibitor)	Type 2 (non-steroidal inhibitor)
First	Testolactone	Aminoglutethimide
Second	Formestane	Fadrozole
Third	Exemestane	Vorozole
	Atamestane	Anastrozole
		Letrozole

Refs. [4,20].

comparing adjuvant letrozole, tamoxifen, and sequential letrozole–tamoxifen therapy for more than 5 years [8]. In the IES, exemestane had a higher incidence of bone fracture and osteoporosis compared with tamoxifen [9]. The LEAP (letrozole, exemestane, and anastrozole pharmacodynamics) trial is Phase I pharmacodynamic study comparing the effects of the AIs, letrozole, exemestane, and anastrozole on the safety parameters such as serum markers of bone formation and resorption in total of 102 healthy postmenopausal women with normal bone mineral density [10]. Results of this study demonstrated that all 3 inhibitors treated for 24 weeks caused an increment of bone resorption marker such as C-telopeptide crosslinks, while only exemestane increased (no significant) the bone formation marker such as bone alkaline phosphatase and propeptides of type 1 collagen [10]. There is a significant decrease in parathyroid hormone with exemestane than with anastrozole reported in this study [10].

Zolendronic acid, which is a potent bisphosphonate, prevents the bone loss in premenopausal women who received adjuvant estrogen suppression therapy. A twin study to Z-FAST [ZOMETA (zolendronic acid)/Femara (letrozole) Adjuvant Synergy Trial; USA and Canada] trial and ZO-FAST (approximately 30 countries outside USA and Canada) trial has been started [11]. The goal of these trials is to investigate how to best combine zolendronic acid with letrozole in postmenopausal women. Patients will be randomized to zolendronic acid either at the initiation of letrozole therapy or after a decrease in T-score below normal, or in the case of a nontraumatic fracture, with a primary end point of change in lumber bone mineral density [11]. Results of this study demonstrated that bisphosphonate therapy in combination with an AIs offers the potential to prevent AI induced bone loss, but its additional costs may provide financial burdens in the great majority of the patients.

3. AIs and bone: experimental studies

3.1. Animal model

Goss et al. reported that steroidal inhibitor, exemestane and its principal metabolite form, 17-hydroexemestane but not non-steroidal inhibitor, letrozole significantly prevented bone loss in ovariectomized (OVX) rats [12,13]. There were several reports regarding the effects of non-steroidal inhibitors on rat bone tissues [14–17]. Both vorozole [14,15] and aminoglutethimide [16] were reported to impair skeletal development and maintenance in growing and/or aged male rats. However, arimidex had no effects on bone tissues in OVX rats [17]. Exemestane and its principal metabolite, 17-hydroexemestane are structurally related to androstenedione and bind to androgen receptor with relatively low affinity compared to natural ligand of 5α-dihydrotestosterone [18]. These finding suggest that exemestane may demonstrate protective effects toward bone tissues through its androgenic actions. However, clinical studies described above could not confirm these findings and suggest that switching from tamoxifen to exemestane results in significant bone loss [19]. Furthermore, very recently, Goss et al. also reported the effects of atamestane, which is a third generation steroidal aromatase inhibitor, on bone tissues of OVX rats [20]. In this report, atamestane significantly prevent bone loss but androgen blocker, flutamide, does not block this prevention [20]. The mechanisms of atamestane's bone protective effects observed in Goss's report have remained largely unclear. Gasser et al. investigated that the effects of the bisphosphonate, zolendronic acid on bone tissues in 8-month-old female rats treated with letrozole [21]. Zolendronic acid protected against bone loss induced by letrozole treatment in a dose dependent manner. This finding is considered a useful model case reflecting clinical trial such as Z-FAST/ZO-FAST trials described above.

3.2. In vitro model

Various studies using human or animal bone tissues [22,23] and osteoblast cell culture using osteosarcoma cells [24,25] demonstrated that aromatase mRNA or protein was detected in osteoblast cells, which play an important role in bone remodeling. Therefore, AIs are considered to effect directly on osteoblast cells. Recently, we reported the direct effects of aromatase inhibitors on osteoblast using osteoblast cell line, hFOB, and osteoblast-like cell lines, Saos-2 and MG-63 [26]. We recently demonstrated that there was a significant increment in the number of the cells treated with steroidal aromatase inhibitor such as exemestane in hFOB and Saos-2 but not in MG-63. Androgen is well known to stimulate osteoblast proliferation [27] and differentiation [28]. Pretreatment with the androgen receptor blocker, flutamide, partially inhibited the effects of exemestane [26]. Non-steroidal aromatase inhibitors such as experimental reagent, aromatase inhibitor I [4-(Imidazolylmethyl)-1-nitro-9H-9-xanthenone; EMD Biosciences, Inc.] [26], and letrozole (personal finding) exerted no effects on osteoblast cell proliferation. Furthermore, first generation of non-steroidal inhibitor, aminoglutethimide significantly diminished the number of cells of hFOB, MG-63, and Saos-2, respectively [26]. Fadrozole was also reported to demonstrate no effects on cell proliferation of human osteoblast-like cell line HOS [29], but relatively high dose (1 μM) of steroidal inhibitor, formestane (4-hydroxyandrostenedione) significantly reduced proliferation of male rat long bone-derived osteoblast-like cells [30].

Bone mass is maintained when the removal of old bone, resorption and the synthesis of new bone, formation performed by osteoclast and osteoblast are balanced (coupled). Osteoclasts,

which are responsible for bone resorption, are target cells of many anti-osteoporosis therapeutic agents such as bisphosphonate of postmenopausal women. Human mononuclear leukemia derived THP-1 cells have been shown to be capable of high rates of aromatase activity, especially following differentiation into osteoclast-like cells with vitamin D treatment [31]. However, it is unclear whether both steroidal and non-steroidal AIs act on osteoclast and osteoclast-like cells directly.

4. Conclusion

Results of many clinical trials compared the effects of AIs on bone tissues with that of tamoxifen. Tamoxifen is a selective estrogen receptor modulator and has a potent anti-estrogenic effect. Tamoxifen has also partial estrogen agonistic effects on uterus as well as bone tissues. Therefore, the treatment with tamoxifen therapy may be related to direct effects on gynecological tissues. AIs are all associated with lower rates of gynecological symptoms and endometrial cancer compared with tamoxifen [7,8]. AIs will replace tamoxifen as the treatment of choice in several type of breast. More than 50 of aromatase inhibition materials such as steroidal, non-steroidal inhibitor, and flavonoids have been discovered [32]. Damages of the bone tissues by the estrogen depletion for aromatase inhibitor administration are unavoidable. However, selection of the hormone therapy that minimizes the damage of bone tissues is important.

References

[1] Thorsen T, Tangen M, Stoa KF. Concentration of endogenous oestradiol as related to oestradiol receptor sites in breast tumor cytosol. Eur J Cancer Clin Oncol 1982;18:333–7.

[2] van Landeghem AA, Poortman J, Nabuurs M, Thijssen JH. Endogenous concentration and subcellular distribution of estrogens in normal and malignant human breast tissue. Cancer Res 1985;45:2900–6.

[3] Sasano H, Harada N. Intratumoral aromatase in human breast, endometrial, and ovarian malignancies. Endocr Rev 1998;19:593–607.

[4] Miller WR, Dixon JM. Endocrine and clinical endpoints of exemestane as neoadjuvant therapy. Cancer Control 2002;9:9–15.

[5] Vanderschueren D, Vandenput L, Boonen S, Lindberg MK, Bouillon R, Ohlsson C. Androgens and bone. Endocr Rev 2004;25:389–425.

[6] Riggs BL, Khosla S, Melton 3rd LJ. A unitary model for involutional osteoporosis: estrogen deficiency causes both type I and type II osteoporosis in postmenopausal women and contributes to bone loss in aging men. J Bone Miner Res 1998;13:763–73.

[7] Howell A, Cuzick J, Baum M, Buzdar A, Dowsett M, Forbes JF, et al. Results of the ATAC (Arimidex, Tamoxifen, Alone or in Combination) trial after completion of 5 years' adjuvant treatment for breast cancer. Lancet 2005;365:60–2.

[8] Thürlimann B, Keshaviah A, Coates AS, Mouridsen H, Mauriac L, Forbes JF, et al. A comparison of letrozole and tamoxifen in postmenopausal women with early breast cancer. N Engl J Med 2005;353:2747–57.

[9] Coombes RC, Hall E, Gibson LJ, Paridaens R, Jassem J, Delozier T, et al. A randomized trial of exemestane after two to three years of tamoxifen therapy in postmenopausal women with primary breast cancer. N Engl J Med 2004;350:1081–92.

[10] McCloskey E, Hannon R, Lakner G, Clack G, Miyamoto A, Eastell R. The letrozole (L), exemestane (E), and anastrozole (A) pharmacodynamics (LEAP) trial: a direct comparison of bone biochemical measurements between aromatase inhibitors (AIs) in healthy postmenopausal womenASCO Annual Meeting Proceedings Part I. J Clin Oncol 2006;24(18S).

[11] Aapro M. Improving bone health in patients with early breast cancer by adding bisphosphonates to letrozole: the Z-ZO-E-ZO-FAST program. Breast 2006;15:S30–40.

[12] Goss PE, Qi S, Josse RG, Pritzker KPH, Mendes M, Hu H, et al. The steroidal aromatase inhibitor exemestane prevent bone loss in ovariectomized rats. Bone 2004;34:384–92.

[13] Goss PE, Qi S, Cheung AM, Hu H, Mendes M, Pritzker KPH. Effects of steroidal aromatase inhibitor exemestane and the nonsteroidal aromatase inhibitor letrozole on bone and lipid metabolism in the ovariectomized rats. Clin Cancer Res 2004;10:5717–23.

[14] Vanderschueren D, van Herck E, Nijs J, Ederveen AG, De Coster R, Bouillon R. Aromatase inhibition impairs skeletal modeling and decreases bone mineral density in growing male rats. Endocrinology 1997;138:2301–7.

[15] Vanderschueren D, Boonen S, Ederveen AG, de Coster R, Van Herck E, Moermans K, et al. Skeletal effects of estrogen deficiency as induced by an aromatase inhibitor in an aged male rat model. Bone 2000;27:611–7.

[16] Boross M, Morava E, Gergely I, Hollo I. Effects of prolonged aminoglutethimid and dehydroepiandrosterone treatment on rat bones. Aktuelle Gerontol 1983;13:15–8.

[17] Lea CK, Flanagan AM. Physiological plasma levels of androgens reduce bone loss in the ovariectomized rat. Am J Physiol 1998;274:E328–35.

[18] Center for Drug Evaluation and Research Application Number NDA 20753 (Exemestane) Medical Review. Food and Drug Administration; 1999.

[19] Jonat W, Hilpert F. Optimizing the use of aromatase inhibitors in adjuvant therapy for postmenopausal patients with hormone-responsive early breast cancer: current and future prospects. J Cancer Res Clin Oncol 2006;132:343–55.

[20] Goss PE, Qi S, Hu H, Cheung AM. The effects of atamestane and toremifene alone and in combination compared with letrozole on bone, serum lipids and the uterus in an ovariectomized rat model. Breast Cancer Res Treat 2007;103:293–302.

[21] Gasser JA, Green JR, Shen V, Ingold P, Rebmann A, Bhatnagar AS, et al. A single intravenous administration of zoledronic acid prevents the bone loss and mechanical compromise induced by aromatase inhibition in rats. Bone 2006;39:787–95.

[22] Sasano H, Uzuki M, Sawai T, Nagura H, Matsunaga G, Kashimoto O, et al. Aromatase in human bone tissue. J Bone Miner Res 1997;12:1416–23.

[23] Schweikert HU, Wolf L, Romalo G. Oestrogen formation from androstenedione in human bone. Clin Endocrinol 1995;43:37–42.

[24] Purohit A, Flanagan AM, Reed MJ. Estrogen synthesis by osteoblast cell lines. Endocrinology 1992;131:2027–9.

[25] Tanaka S, Haji M, Nishi Y, Yanase T, Takayanagi R, Nawata H. Aromatase activity in human osteoblast-like osteosarcoma cell. Calcif Tissue Int 1993;52:107–9.

[26] Miki Y, Suzuki T, Hatori M, Igarashi K, Aisaki K, Kanno J, et al. Effects of aromatase inhibitors on human osteoblast and osteoblast–like cells: a possible androgenic bone protective effects induced by exemestane. Bone 2007;40:876–87.

[27] Kasperk CH, Wergedal JE, Farley JR, Linkhart TA, Turner RT, Baylink DJ. Androgens directly stimulate proliferation of bone cells *in vitro*. Endocrinology 1989;124:1576–8.

[28] Kasperk C, Fitzsimmons R, Strong D, Mohan S, Jennings J, Wergedal J, et al. Studies of the mechanism by which androgens enhance mitogenesis and differentiation in bone cells. J Clin Endocrinol Metab 1990;71:1322–9.

[29] Morioka M, Shimodaira K, Kuwano Y, Fujikawa H, Saito H, Yanaihara T. Effect of interleukin-1beta on aromatase activity and cell proliferation in human osteoblast-like cells (HOS). Biochem Biophys Res Commun 2000;268:60–4.

[30] Damien E, Price JS, Lanyon LE. Mechanical strain stimulates osteoblast proliferation through the estrogen receptor in males as well as females. J Bone Miner Res 2000;15:2169–77.

[31] Jakob F, Hormann D, Seufert J, Schneider D, Kohrle J. Expression and regulation of aromatase cytochrome P450 in THP-1 human myeloid leukemia cells. Mol Cell Endocrinol 1995;110:27–33.

[32] Seralini G, Moslemi S. Aromatase inhibitors: past, present and future. Mol Cell Endocrinol 2001;178:117–31.

LETTERS

Dioxin receptor is a ligand-dependent E3 ubiquitin ligase

Fumiaki Ohtake[1,2], Atsushi Baba[2], Ichiro Takada[2], Maiko Okada[2], Kei Iwasaki[1], Hiromi Miki[2], Sayuri Takahashi[2,3], Alexander Kouzmenko[1,2], Keiko Nohara[4], Tomoki Chiba[5], Yoshiaki Fujii-Kuriyama[6,7] & Shigeaki Kato[1,2]

Fat-soluble ligands, including sex steroid hormones and environmental toxins, activate ligand-dependent DNA-sequence-specific transcriptional factors that transduce signals through target-gene-selective transcriptional regulation[1]. However, the mechanisms of cellular perception of fat-soluble ligand signals through other target-selective systems remain unclear. The ubiquitin–proteasome system regulates selective protein degradation, in which the E3 ubiquitin ligases determine target specificity[2–4]. Here we characterize a fat-soluble ligand-dependent ubiquitin ligase complex in human cell lines, in which dioxin receptor (AhR)[5–9] is integrated as a component of a novel cullin 4B ubiquitin ligase complex, CUL4B^{AhR}. Complex assembly and ubiquitin ligase activity of CUL4B^{AhR} *in vitro* and *in vivo* are dependent on the AhR ligand. In the CUL4B^{AhR} complex, ligand-activated AhR acts as a substrate-specific adaptor component that targets sex steroid receptors for degradation. Thus, our findings uncover a function for AhR as an atypical component of the ubiquitin ligase complex and demonstrate a non-genomic signalling pathway in which fat-soluble ligands regulate target-protein-selective degradation through a ubiquitin ligase complex.

The transcriptional regulatory system and the ubiquitin–proteasome system are two major target-selective systems that control intracellular protein levels. This target selectivity depends on the recognition of specific DNA elements by sequence-specific transcription factors[1] and the recognition of degradation substrates by E3 ubiquitin ligases[2–4]. These transcription factors and ligases serve primarily as specific adaptors that subsequently recruit transcriptional co-regulators and E2 ubiquitin-conjugating enzymes, respectively, to appropriate targets. The selective biological effects of fat-soluble ligands have been reported to be mediated by two classes of sequence-specific transcription factors, nuclear receptors[1] and arylhydrocarbon receptor (AhR) belonging to the basic helix–loop–helix (bHLH)/Per-Arnt-Sim (PAS) family[5–9].

AhR ligands modulate oestrogen and sex hormone, signalling both positively and negatively[8,10–13]. Functional impairments of male and female reproductive organs in AhR-deficient mice indicate the possible importance of AhR in sex hormone signalling[10,14]. Different AhR agonists[9], including 3-methylcholanthrene (3MC) and 2,3,7,8-tetrachlordibenzo-*p*-dioxin (TCDD), modulate oestrogen-dependent oestrogen receptor (ER)-α transactivation through the association of activated AhR/Arnt with ER-α[15]. Similarly, the transcriptional activity of nuclear androgen receptor (AR) was modulated by association with activated AhR (Supplementary Fig. S2a). However, ligand-bound AhR did not block oestrogen-induced co-activator recruitment on the oestrogen-responsive promoter (Supplementary Fig. S2b). This implies another mode of function for ligand-activated AhR beyond transcriptional regulation.

On activation of AhR by 3MC, we observed that protein levels of endogenous ER-α (in mammary tumour MCF-7 cells), ER-β (in ovarian tumour KGN cells) and AR (in prostate cancer LNCaP cells) were drastically decreased (Fig. 1a–c, and Supplementary Fig. 3a) without a change in messenger RNA levels (data not shown), irrespective of the presence of their cognate hormones. Other AhR agonists[9] (namely β-naphthoflavone (β-NF), environmental toxins such as TCDD and benzo[a]pyrene, and the endogenous metabolite indirubin) were similarly effective in protein degradation for ER-α (Fig. 1b) and ER-β/AR (data not shown), in agreement with a previous report on downregulated levels of uterine ER-α protein in rats treated with TCDD[16]. An AhR partial agonist/antagonist α-naphthoflavone (α-NF) was unable to accelerate the degradation of either AhR or ER-α (Fig. 1b, and Supplementary Fig. S3b).

AhR ligand-induced degradation (Fig. 1a–c) and functional repression (Supplementary Fig. S2c, d) of sex steroid receptors were abrogated in the presence of a proteasome inhibitor MG132. Consistently, poly-ubiquitination of ER-α was promoted by the activated AhR regardless of the presence of oestrogen (Fig. 1d, and Supplementary Fig. S3c). Pulse-chase kinetic analysis indicated that 3MC-induced degradation of ER-α was coupled to that of AhR[8,17,18] (Supplementary Fig. S3d). Moreover, the self-ubiquitination activity of the ligand-bound AhR immunocomplex was detected in an E1/E2-dependent manner (Supplementary Fig. S3e). Together with 3MC-dependent recognition of sex steroid receptors by AhR[8,12,13,15], these properties of AhR resemble those of classical adaptor components of the E3 ubiquitin ligase complexes, such as F-box proteins[3] or von Hippel–Lindau protein[19]. We therefore reasoned that activated AhR might act as an E3 ubiquitin ligase complex component.

To address this idea, AhR-containing complexes were purified from HeLa cells expressing Flag–AhR treated with 3MC or α-NF[15,20]. AhR formed large complexes in the presence of 3MC (Supplementary Fig. S4a–c). Further purification revealed five major 3MC-dependent complexes containing AhR (Fig. 1e). Complexes A and C contained well-known co-activators TRAP220/DRIP205/Med220 and p300 (ref. 1) (Supplementary Fig. S4d, e). Endogenous ER-α was detected in complexes B and C; however, ubiquitinated components were seen only in complex B (Fig. 1f, g).

Complex B was composed of the ubiquitin ligase core components cullin 4B (CUL4B)[3,21,22], damaged-DNA-binding protein 1 (DDB1)[23–27] and Rbx1 (Roc1)[3], together with subunits of the proteasomal 19S regulatory particle (19S RP), Arnt and transducin-β-like 3 (TBL3) (Fig. 1h). These components eluted with AhR in the presence of 3MC but not in the presence of α-NF (Fig. 1i, and Supplementary Fig. S4f). Neither CUL4A nor known substrate-specific adaptor components of CUL4A, such as DDB2, CSA and DET1[23,24], were present

[1]ERATO, Japan Science and Technology Agency, 4-1-8 Honcho, Kawaguchi, Saitama 332-0012, Japan. [2]Institute of Molecular and Cellular Biosciences, University of Tokyo, 1-1-1 Yayoi, Bunkyo-ku, Tokyo 113-0032, Japan. [3]Department of Urology, Faculty of Medicine, University of Tokyo, 7-3-1 Hongo, Bunkyo-ku, 113-8655, Japan. [4]National Institute for Environmental Studies, Tsukuba, Ibaraki 305-8506, Japan. [5]Graduate School of Life and Environmental Sciences, and [6]TARA Center, University of Tsukuba, 1-1-1 Tennodai Tsukuba, 305-8577, Japan. [7]SORST, Japan Science and Technology Agency, 4-1-8 Honcho, Kawaguchi, Saitama 332-0012, Japan.

in the AhR–CUL4B complex. As the cullin amino terminus binds adaptor components and the carboxy terminus interacts with an E2 enzyme-binding subunit Rbx1 (ref. 3), we performed tandem purification of the AhR–CUL4B complex with glutathione *S*-transferase (GST)-tagged CUL4B-N (N-terminal domain of CUL4B) and Flag–AhR. This led to the identification of a core complex consisting of five components: DDB1, AhR, Arnt, TBL3 and CUL4B (Fig. 1j). Together with Rbx1, this complex is denoted by $CUL4B^{AhR}$.

Immunoprecipitation of AhR together with endogenous CUL4B from MCF-7 and LNCaP cells was observed only in the presence of 3MC (Fig. 2a, b). Consistently, ligand-dependent co-localization of AhR with CUL4 was seen in MCF-7 cells (Fig. 2c). Whereas CUL4B seemed to act as a scaffold mediating DDB1–TBL3 and AhR–DDB1 interactions in $CUL4B^{AhR}$ (Fig. 2d, lane 4), ligand-activated AhR induced the assembly of complex components (Fig. 2d, lanes 1–3). DDB1 did not bridge CUL4B association with TBL3 or AhR, apparently because of the absence of the signature WDXR/DWD box[22,25–27] of either TBL3 or AhR, which is essential for DDB1 binding (Fig. 2d, lane 5, and Supplementary Fig. S5a). Consistently, specific and 3MC-dependent interaction of the conserved C-terminal acidic domain of AhR with the N-terminal region of CUL4B, but not with DDB1, was observed in a GST pulldown assay (Supplementary Figs S5b and S6). Because a constitutively active AhR mutant (AhRΔPASB)[9] interacted with CUL4B in the absence of ligand (Supplementary Fig. S5b), ligand-dependent structural alteration presumably induces AhR–CUL4B interaction. An AhR mutant lacking the CUL4B-binding

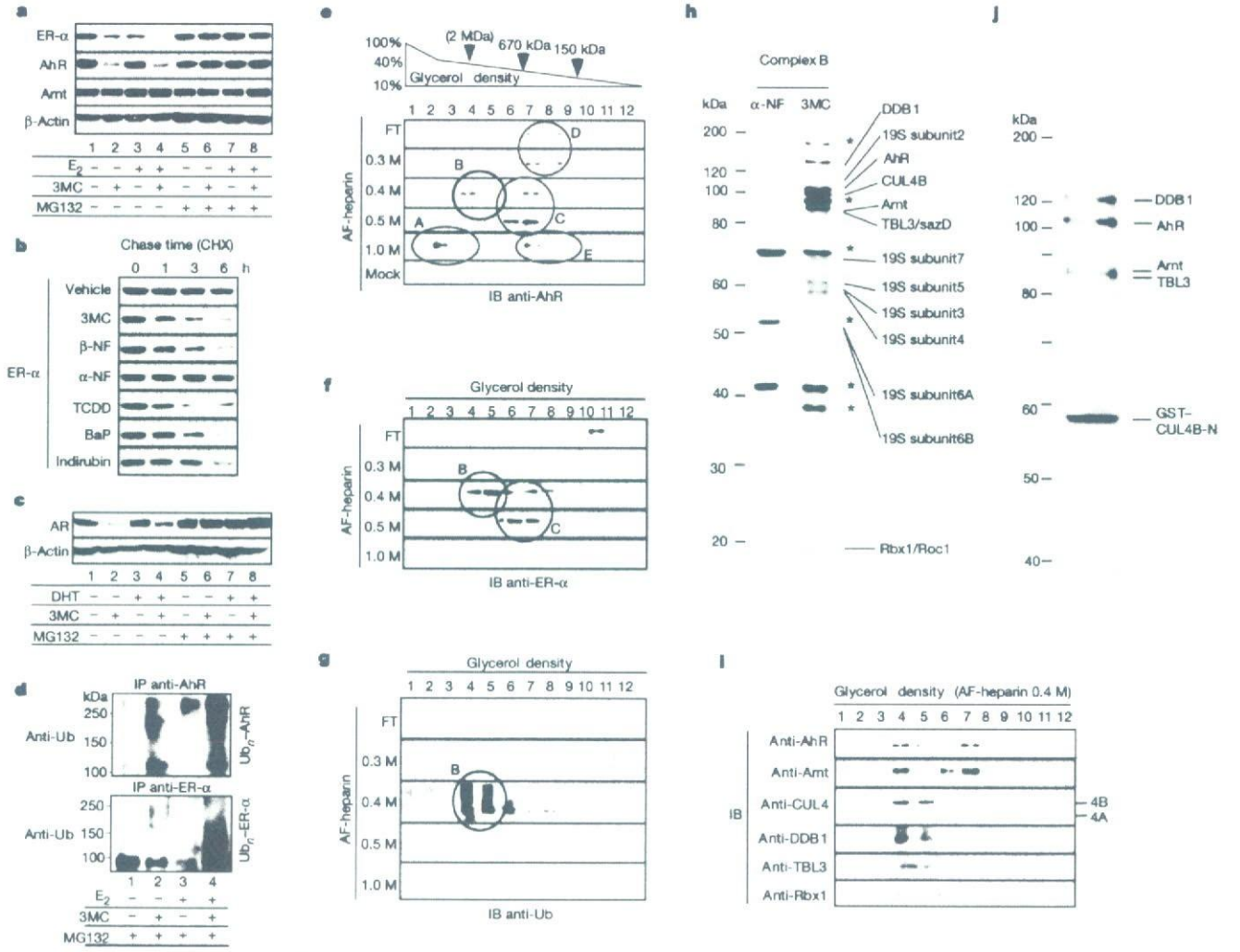

Figure 1 | Activated AhR acts as an E3 ubiquitin ligase. **a–c**, AhR-ligand-induced proteasomal degradation of ER-α (**a**, **b**) and AR (**c**). MCF-7 cells (**a**, **b**) and LNCaP cells (**c**) were incubated as indicated with E_2 (10 nM), DHT (10 nM) and/or 3MC (1 μM), β-NF (1 μM), benzo[a]pyrene (BaP; 100 nM), TCDD (10 nM), indirubin (10 nM) and α-NF (1 μM) in the presence or absence of MG132 (10 μM) and cycloheximide (CHX; 5 μM) for 3 h (**a**, **c**) or the indicated durations (**b**). Cell lysates were subjected to western blotting with specified antibodies. **d**, AhR-ligand-induced ubiquitination of ER-α. MCF-7 cells were incubated with the indicated ligands for 6 h. Western blots were subjected to dark exposure to detect poly-ubiquitinated forms of the receptors. IP, immunoprecipitation; Ub, ubiquitin. **e**, **f**, Biochemical separation and identification of AhR-associated complexes. Flag–AhR-associated proteins in the presence of 3MC or α-NF from HeLa cells stably expressing Flag–AhR were first fractionated by glycerol-density-gradient centrifugation (top, fractions 1–12), and then separated by Toyopearl AF-heparin column chromatography with the indicated KCl concentrations (FT, 1.0 M KCl). Samples from the 3MC-treated cells were resolved into five distinct complexes. IB, immunoblotting. **g**, Components of an AhR-associated complex are highly ubiquitinated. Western blots with anti-ubiquitin antibody. **h**, Identification of AhR-associated CUL4B ubiquitin ligase complex components. Components from complex B in **e** (fractions 4 and 5 from the glycerol-density-gradient centrifugation, eluted from an AF-heparin column at 0.4 M KCl) were resolved by SDS–PAGE, silver-stained and identified by matrix-assisted laser desorption ionization–time-of-flight MS analysis. **i**, Co-elution of the complex B components as a large complex. **j**, Association of activated AhR with the CUL4B complex. The $CUL4B^{AhR}$ complex from Flag–AhR-expressing HeLa cells treated with 3MC was affinity purified with GST-tagged N-terminal domain of CUL4B followed by anti-Flag antibody column fractionation.

acidic domain (AhRΔacid; Supplementary Fig. S6a) was indeed unable to promote ER-α ubiquitination *in vivo*, although the mutant retained 3MC-dependent transactivation function (Supplementary Fig. S5c). This indicates that the ubiquitin ligase function of AhR is independent of its transactivation function.

With two separately prepared components of recombinant AhR and CUL4B/DDB1/Rbx1 purified from *Spodoptera frugiperda* (Sf9) cells (Supplementary Fig. S7a), complex assembly *in vitro* was also dependent on 3MC (Fig. 2e). Furthermore, by *in vitro* ubiquitination assay (Supplementary Fig. S7b), the E3 ubiquitin ligase activity of $CUL4B^{AhR}$ for ER-α was dependent on 3MC but not on 17β-oestradiol (E_2) (Fig. 2f). These data indicate that both the complex assembly and the ubiquitin ligase activity of $CUL4B^{AhR}$ may be dependent on AhR agonists.

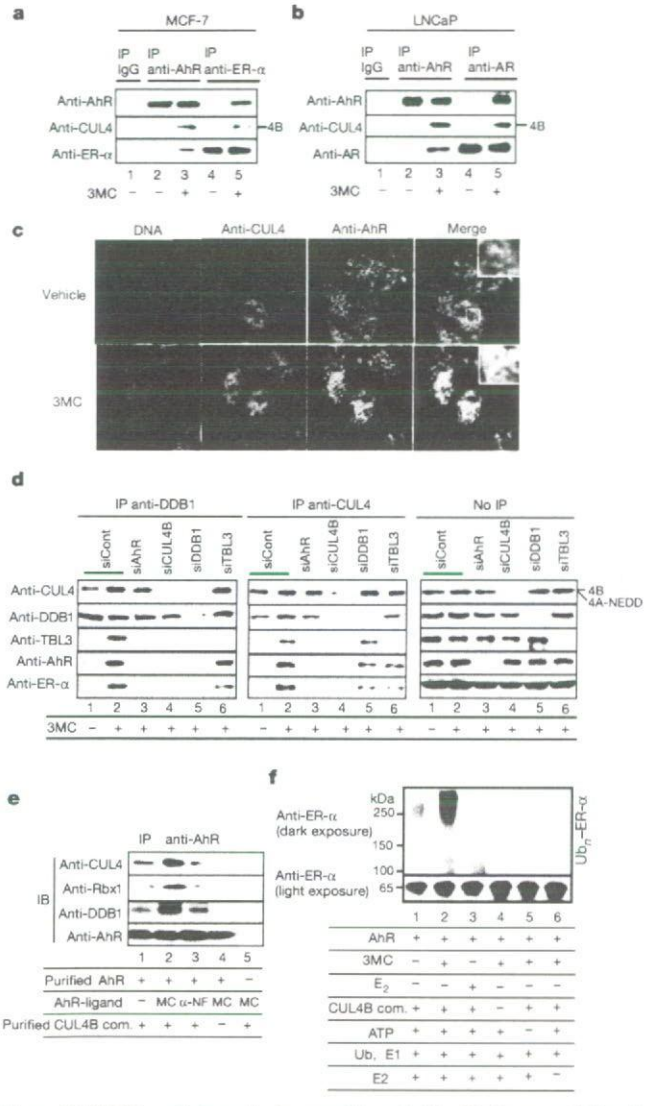

Figure 2 | AhR ligand-dependent assembly and ubiquitin ligase activity of $CUL4B^{AhR}$. **a**, **b**, 3MC-dependent association of endogenous CUL4B and AhR with ER-α and AR. Co-immunoprecipitation analyses from MCF-7 (**a**) and LNCaP (**b**) cells incubated with ligand and MG132 for 2 h. IP, immunoprecipitation. **c**, 3MC-dependent co-localization of AhR with CUL4. MCF-7 cells incubated with 3MC and MG132 for 2 h were immunostained with the indicated antibodies. **d**, Formation of the $CUL4B^{AhR}$ complex. MCF-7 cells were transfected with specified short interfering RNAs (siRNAs) for 48 h, treated with 3MC and MG132 for 2 h, and immunoprecipitated with the indicated antibodies. **e**, Assembly of the CUL4B complex components with AhR is dependent on 3MC *in vitro*. Immunoprecipitation with anti-AhR antibodies of the indicated recombinant CUL4B complex components (CUL4B com.) was observed only in the presence of 3MC. IB, immunoblotting. **f**, $CUL4B^{AhR}$ ubiquitinates ER-α *in vitro*. ER-α protein was incubated with and without recombinant $CUL4B^{AhR}$ E3 complex components, ubiquitin (Ub), ATP, E1 and E2 enzymes as indicated, then subjected to western blotting.

We then examined whether the recognition of sex steroid receptors for 3MC-dependent ubiquitination is indeed mediated by AhR. Co-immunoprecipitation analyses indicated that ligand-activated AhR was required for the recruitment of ER-α (Fig. 2a, d) or AR (Fig. 2b, and data not shown) to $CUL4B^{AhR}$. TBL3 and DDB1 did not seem essential for ER-α recruitment but stabilized the association of ER-α with $CUL4B^{AhR}$ (Fig. 2d). Moreover, knockdown of $CUL4B^{AhR}$ components (Supplementary Fig. S8) impaired the 3MC-induced ubiquitination and degradation of ER-α (Fig. 3a–d, and Supplementary Fig. S9a, b) and AR (Fig. 3e, Supplementary Fig. S9c and data not shown), and abolished the AhR-ligand-induced repression of ER-α transactivation (Supplementary Fig. S10a). Recognition of ER-α by activated AhR was retained, but ubiquitination of AhR-bound ER-α was abrogated, by knockdown of the other $CUL4B^{AhR}$ components (Fig. 3d). An ER-α ΔA/B mutant[15] that lacks interaction with AhR, and an ER-α K7R mutant in which seven lysine residues had been replaced with arginine (Supplementary Fig. S6b), were resistant to AhR-dependent ubiquitination and transrepression (Fig. 3f, and Supplementary Fig. S10b). Taken together, these data suggest that ligand-activated AhR functions as a substrate-specific adaptor component of $CUL4B^{AhR}$. AhR is therefore a unique and atypical substrate-specific component of a cullin-based E3 complex, because AhR bears no known interaction motif with cullin complexes yet associates directly with CUL4B. Ubiquitination of ER-α-associated AhR was similarly abolished by the knockdown, and the overall ubiquitination and degradation of AhR[8,17,18] were partly affected (Supplementary Fig. S11a, b). This implies the existence of $CUL4B^{AhR}$-dependent (self-ubiquitination[3]) and $CUL4B^{AhR}$-independent pathways for AhR degradation.

Human ER-α (hER-α) degradation is reportedly accelerated by the binding of E_2 (ref. 1) or the phosphorylation of Ser 118 (ref. 28), whereas a partial antagonist, tamoxifen, has been shown to stabilize ER-α[1]. Nevertheless, 3MC-activated AhR efficiently induced the ubiquitination and subsequent degradation of tamoxifen-bound ER-α and ER-α-S118A mutant (Fig. 3f). Reciprocally, AhR was dispensable for E_2-dependent ER-α degradation (Supplementary Fig. S11c). These results indicate that the $CUL4B^{AhR}$ system may act independently of innate protein degradation system(s) for ER-α. XAP2/ARA9/AIP[7,8,17], a chaperone that modulates the stability of unliganded AhR, seemed unlikely to mediate the accelerated degradation of ER-α by activated AhR (Supplementary Fig. S11d).

Last, we addressed the physiological significance of $CUL4B^{AhR}$ for sex hormone signalling in intact animals. Injection with either 3MC (Fig. 4a) or β-NF (Fig. 4c) did not affect the expression of ER-α or AR mRNA (data not shown) but caused a decrease in protein levels of uterine ER-α in ovariectomized female wild-type mice and of prostate AR in castrated male wild-type mice (Fig. 4b) regardless of their treatment with cognate sex hormones. However, AhR deficiency ($AhR^{-/-}$ mice)[9,14] abolished such effects of AhR ligands but did not affect the modulation of stability of sex steroid receptors by their respective hormones (Fig. 4a, b). As a result of reduced sex steroid receptor levels after pretreatment with 3MC, E_2-dependent induction of c-*fos* in the uterus[15] and dihydrotestosterone (DHT)-dependent induction of *Probasin* in the prostate[10] were severely impaired (Fig. 4a, b). Cellular proliferation and gene induction in response to sex hormones in primary cultured epithelial cells from normal mouse uterus and prostate were consistently suppressed by 3MC (Supplementary Fig. S12a, b) and β-NF (Supplementary Fig. S12c), but no effect was detected in $AhR^{-/-}$ cells (Supplementary Fig. S12a, b). The significance of $CUL4B^{AhR}$ complex components in the AhR-mediated suppression of sex hormone effects

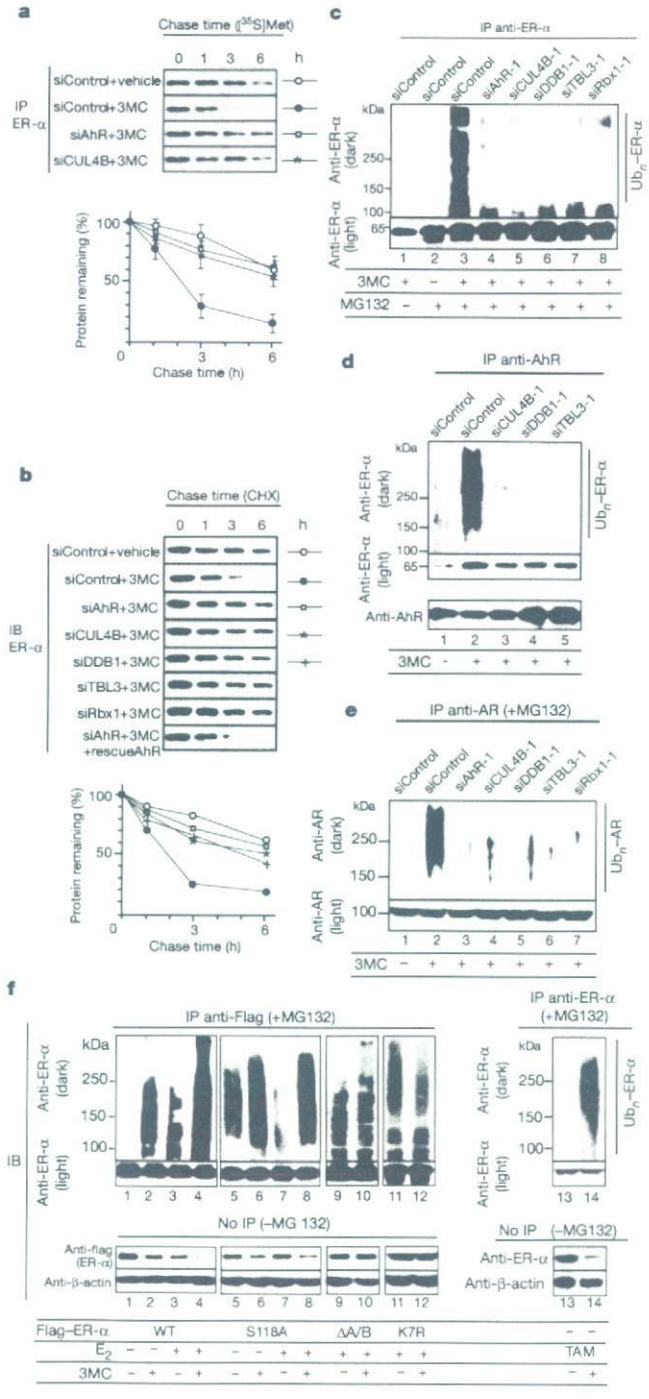

Figure 3 | Activated AhR is a substrate-specific adaptor component of the CUL4B^{AhR} complex. a–c, Components of CUL4B^{AhR} are required for 3MC-dependent ubiquitination and degradation of ER-α. MCF-7 cells were transfected with indicated siRNAs for 48 h, then used in pulse-chase analysis as in Supplementary Fig. S3d (**a**), in cycloheximide (CHX) chasing (**b**) and in the *in vivo* ubiquitination assay with ligand incubation for 6 h (**c**). All values are shown as means ± s.d. ($n = 3$) (**a**) or as means ($n = 3$) (**b**). The knockdown efficiency in the same lysates was confirmed in Supplementary Fig. S9a. IB, immunoblotting; IP, immunoprecipitation. **d**, AhR is the substrate-specific adaptor in the targeting of ER-α by CUL4B^{AhR}. MCF-7 cells transfected with the indicated siRNAs were lysed in TNE buffer and immunoprecipitated with anti-AhR antibody in the presence of MG132. Ubiquitination of the ER-α co-immunoprecipitated with AhR was detected by western blotting. **e**, LNCaP cells were subjected to the same analysis as in **a–c**. **f**, AhR-ligand-induced ER-α ubiquitination requires intact lysine residues and is independent of oestrogen binding or S118 phosphorylation of hER-α. Intact MCF-7 cells (right) or cells transfected with Flag–hER-α, AhR and their derivatives (left) were treated with the indicated ligands in the presence (top) or absence (bottom) of MG132 for 6 h, then subjected to western blotting. TAM, tamoxifen; WT, wild type.

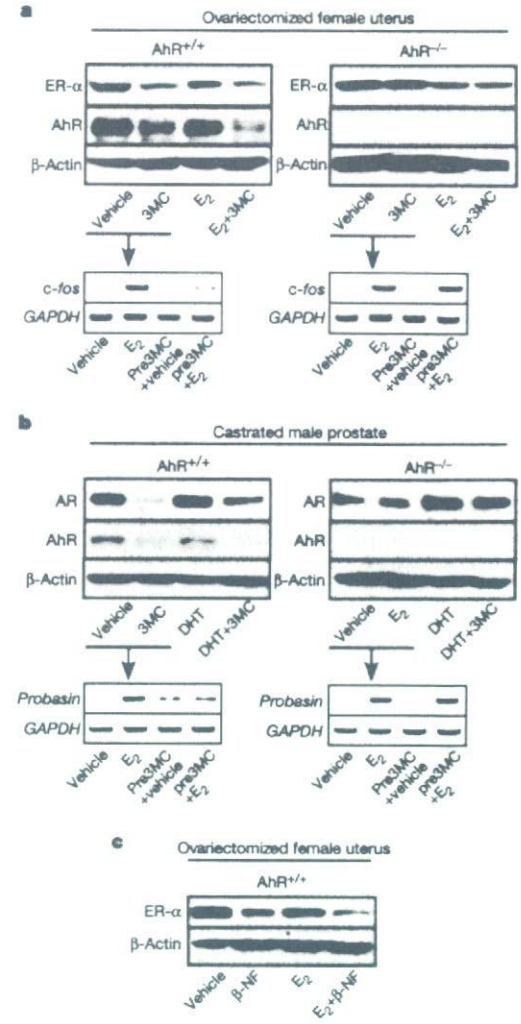

Figure 4 | Ligand-dependent ubiquitin ligase function of AhR *in vivo*. **a, b**, AhR activation enhances the degradation of ER-α and AR *in vivo*. Top: nine-week-old ovariectomized female mice (**a**) or castrated male mice (**b**) of the indicated genotypes were injected with vehicle or indicated ligands. After 4 h, uterus (**a**) or ventral prostate (**b**) was isolated and subjected to western blotting. Bottom: mice pretreated with vehicle or 3MC for 8 h were injected with either vehicle or E_2 (**a**), or DHT (**b**). After 4 h, the uterus or prostate was isolated for reverse transcriptase PCR. GAPDH, glyceraldehyde-3-phosphate dehydrogenase. **c**, Other AhR agonists produce a similar effect on oestrogen signalling to that of 3MC.

(Supplementary Fig. S12a, b) and the promotion of ER-α degradation in uterine cells (Supplementary Fig. S12d) was verified by knockdown of the components.

Here we have shown that a known sequence-specific transcription factor AhR acts as a ligand-dependent CUL4B-based E3 ubiquitin ligase for selectively targeting sex steroid receptors to bring about accelerated protein degradation. The transcription and ubiquitination functions of AhR seem to be responsible for a distinct set of biological events caused by endogenous and exogenous AhR ligands. In ubiquitin ligase complexes, substrate recognition by known

substrate-specific components is generally evoked by substrate modifications[2–4]. However, the recognition and subsequent ubiquitination of sex steroid receptors by AhR requires dioxin-type compounds as ligands but does not require the phosphorylation or ligand binding of sex steroid receptors. We have therefore shown that fat-soluble ligands directly control the function of a ubiquitin ligase complex for targeted protein destruction in animals (see Supplementary Fig. S1). In plants, auxin was recently found to control protein destruction through the auxin receptor SCF^{TIR1} (refs 29, 30). However, whereas SCF^{TIR1} is regulated by ligand-dependent substrate recognition by TIR1, $CUL4B^{AhR}$ is primarily regulated by the assembly of a ligand-dependent complex as well as substrate recognition. Considered together, ubiquitin-ligase-based perception mechanisms of fat-soluble ligands may be diverse in different species. It is possible that other nuclear receptors and binding proteins for fat-soluble ligands also serve as key components of ubiquitin ligases to mediate a non-genomic pathway of fat-soluble ligands to regulate target-protein-selective destruction.

METHODS

More detailed descriptions of all materials and methods are supplied in the Supplementary Information.

Biochemical purification and separation of AhR-associated complexes. The nuclear extracts preparation, anti-Flag affinity purification and mass spectrometry were performed as described previously[15,20]. For purification of the core $CUL4B^{AhR}$ complex, the nuclear extracts were first bound to the GST–CUL4B-N (amino acid residues 1–318) columns before being loaded on anti-Flag columns[20].

***In vitro* ubiquitination assay.** The *in vitro* ubiquitination assay was performed as described previously[23]. Purified Flag–AhR (0.2 μg) was incubated either with 3MC (10 μM) or vehicle (dimethylsulphoxide) for 30 min at 25 °C, then mixed with Flag–CUL4B/DDB1/Rbx1 complex (0.2 μg), and after further incubation for 30 min at 25 °C the substrate, ER-α (Calbiochem), was added.

Plasmids, antibodies, immunoprecipitation, *in vivo* ubiquitination, pulse-chasing, ligand responses in mice, and RNA-mediated interference experiments. Detailed methods used in this study can be found in the Supplementary Information.

Received 13 December 2006; accepted 16 February 2007.

1. McKenna, N. J. & O'Malley, B. W. Combinatorial control of gene expression by nuclear receptors and coregulators. *Cell* **108**, 465–474 (2002).
2. Hershko, A. & Ciechanover, A. The ubiquitin system. *Annu. Rev. Biochem.* **67**, 425–479 (1998).
3. Deshaies, R. J. SCF and Cullin/Ring H2-based ubiquitin ligases. *Annu. Rev. Cell Dev. Biol.* **15**, 435–467 (1999).
4. Harper, J. W. A phosphorylation-driven ubiquitination switch for cell-cycle control. *Trends Cell Biol.* **12**, 104–107 (2002).
5. Poellinger, L. Mechanistic aspects—the dioxin (aryl hydrocarbon) receptor. *Food Addit. Contam.* **17**, 261–266 (2000).
6. Hankinson, O. The aryl hydrocarbon receptor complex. *Annu. Rev. Pharmacol. Toxicol.* **35**, 307–340 (1995).
7. Swanson, H. I. & Bradfield, C. A. The AH-receptor: genetics, structure and function. *Pharmacogenetics* **3**, 213–230 (1993).
8. Carlson, D. B. & Perdew, G. H. A dynamic role for the Ah receptor in cell signaling? Insights from a diverse group of Ah receptor interacting proteins. *J. Biochem. Mol. Toxicol.* **16**, 317–325 (2002).
9. Mimura, J. & Fujii-Kuriyama, Y. Functional role of AhR in the expression of toxic effects by TCDD. *Biochim. Biophys. Acta* **1619**, 263–268 (2003).
10. Lin, T. M. *et al.* Effects of aryl hydrocarbon receptor null mutation and in utero and lactational 2,3,7,8-tetrachlorodibenzo-*p*-dioxin exposure on prostate and seminal vesicle development in C57BL/6 mice. *Toxicol. Sci.* **68**, 479–487 (2002).
11. Brunnberg, S. *et al.* The basic helix–loop–helix-PAS protein ARNT functions as a potent coactivator of estrogen receptor-dependent transcription. *Proc. Natl Acad. Sci. USA* **100**, 6517–6522 (2003).
12. Matthews, J., Wihlen, B., Thomsen, J. & Gustafsson, J. A. Aryl hydrocarbon receptor-mediated transcription: ligand-dependent recruitment of estrogen receptor α to 2,3,7,8-tetrachlorodibenzo-*p*-dioxin-responsive promoters. *Mol. Cell. Biol.* **25**, 5317–5328 (2005).
13. Beischlag, T. V. & Perdew, G. H. ER α-AHR-ARNT protein–protein interactions mediate estradiol-dependent transrepression of dioxin-inducible gene transcription. *J. Biol. Chem.* **280**, 21607–21611 (2005).
14. Baba, T. *et al.* Intrinsic function of the aryl hydrocarbon (dioxin) receptor as a key factor in female reproduction. *Mol. Cell. Biol.* **25**, 10040–10051 (2005).
15. Ohtake, F. *et al.* Modulation of oestrogen receptor signalling by association with the activated dioxin receptor. *Nature* **423**, 545–550 (2003).
16. Romkes, M., Piskorska-Pliszczynska, J. & Safe, S. Effects of 2,3,7,8-tetrachlorodibenzo-*p*-dioxin on hepatic and uterine estrogen receptor levels in rats. *Toxicol. Appl. Pharmacol.* **87**, 306–314 (1987).
17. Davarinos, N. A. & Pollenz, R. S. Aryl hydrocarbon receptor imported into the nucleus following ligand binding is rapidly degraded via the cytosplasmic proteasome following nuclear export. *J. Biol. Chem.* **274**, 28708–28715 (1999).
18. Roberts, B. J. & Whitelaw, M. L. Degradation of the basic helix–loop–helix/Per-ARNT-Sim homology domain dioxin receptor via the ubiquitin/proteasome pathway. *J. Biol. Chem.* **274**, 36351–36356 (1999).
19. Maxwell, P. H. *et al.* The tumour suppressor protein VHL targets hypoxia-inducible factors for oxygen-dependent proteolysis. *Nature* **399**, 271–275 (1999).
20. Kitagawa, H. *et al.* The chromatin-remodeling complex WINAC targets a nuclear receptor to promoters and is impaired in Williams syndrome. *Cell* **113**, 905–917 (2003).
21. Zhong, W., Feng, H., Santiago, F. E. & Kipreos, E. T. CUL-4 ubiquitin ligase maintains genome stability by restraining DNA-replication licensing. *Nature* **423**, 885–889 (2003).
22. Higa, L. A. *et al.* CUL4–DDB1 ubiquitin ligase interacts with multiple WD40-repeat proteins and regulates histone methylation. *Nature Cell Biol.* **8**, 1277–1283 (2006).
23. Groisman, R. *et al.* The ubiquitin ligase activity in the DDB2 and CSA complexes is differentially regulated by the COP9 signalosome in response to DNA damage. *Cell* **113**, 357–367 (2003).
24. Wertz, I. E. *et al.* Human De-etiolated-1 regulates c-Jun by assembling a CUL4A ubiquitin ligase. *Science* **303**, 1371–1374 (2004).
25. Jin, J., Arias, E. E., Chen, J., Harper, J. W. & Walter, J. C. A family of diverse Cul4-Ddb1-interacting proteins includes Cdt2, which is required for S phase destruction of the replication factor Cdt1. *Mol. Cell* **23**, 709–721 (2006).
26. Angers, S. *et al.* Molecular architecture and assembly of the DDB1–CUL4A ubiquitin ligase machinery. *Nature* **443**, 590–593 (2006).
27. He, Y. J., McCall, C. M., Hu, J., Zeng, Y. & Xiong, Y. DDB1 functions as a linker to recruit receptor WD40 proteins to CUL4–ROC1 ubiquitin ligases. *Genes Dev.* **20**, 2949–2954 (2006).
28. Valley, C. C. *et al.* Differential regulation of estrogen-inducible proteolysis and transcription by the estrogen receptor alpha N terminus. *Mol. Cell. Biol.* **25**, 5417–5428 (2005).
29. Dharmasiri, N., Dharmasiri, S. & Estelle, M. The F-box protein TIR1 is an auxin receptor. *Nature* **435**, 441–445 (2005).
30. Kepinski, S. & Leyser, O. The *Arabidopsis* F-box protein TIR1 is an auxin receptor. *Nature* **435**, 446–451 (2005).

Supplementary Information is linked to the online version of the paper at www.nature.com/nature.

Acknowledgements We thank K. Tanaka, C. K. Glass, J. Yanagisawa, Y. Gotoh and J. Mimura for comments; S. Murata, T. Matsuda, T. Suzuki and Y. Tateishi for providing materials; T. Matsumoto, M. Igarashi and S. Fujiyama for technical assistance; and H. Higuchi for manuscript preparation. This work was supported in part by the Program for Promotion of Basic Research Activities for Innovative Biosciences (PROBRAIN) and priority areas from the Ministry of Education, Culture, Sports, Science and Technology (to Y.F.-K. and S.K.).

Author Contributions F.O., T.C., Y.F.-K. and S.K. designed the experiments. F.O., A B., M.O., K I., H.M., S.T. and I. T. performed the experiments. F.O., A.K. and S.K. wrote the paper.

Author Information Reprints and permissions information is available at www.nature.com/reprints. The authors declare no competing financial interests. Correspondence and requests for materials should be addressed to S.K. (uskato@mail.ecc.u-tokyo.ac.jp).

nature
cell biology

A histone lysine methyltransferase activated by non-canonical Wnt signalling suppresses PPAR-γ transactivation

Ichiro Takada[1], Masatomo Mihara[1,3], Miyuki Suzawa[1], Fumiaki Ohtake[1,2], Shinji Kobayashi[1,2], Mamoru Igarashi[1], Min-Young Youn[1], Ken-ichi Takeyama[1], Takashi Nakamura[1,2], Yoshihiro Mezaki[1], Shinichiro Takezawa[1], Yoshiko Yogiashi[1], Hirochika Kitagawa[1], Gen Yamada[4], Shinji Takada[5], Yasuhiro Minami[6], Hiroshi Shibuya[7], Kunihiro Matsumoto[8] and Shigeaki Kato[1,2,9]

Histone modifications induced by activated signalling cascades are crucial to cell-lineage decisions. Osteoblast and adipocyte differentiation from common mesenchymal stem cells is under transcriptional control by numerous factors. Although PPAR-γ (peroxisome proliferator activated receptor-γ) has been established as a prime inducer of adipogenesis, cellular signalling factors that determine cell lineage in bone marrow remain generally unknown. Here, we show that the non-canonical Wnt pathway through CaMKII–TAK1–TAB2–NLK transcriptionally represses PPAR-γ transactivation and induces Runx2 expression, promoting osteoblastogenesis in preference to adipogenesis in bone marrow mesenchymal progenitors. Wnt-5a activates NLK (Nemo-like kinase), which in turn phosphorylates a histone methyltransferase, SETDB1 (SET domain bifurcated 1), leading to the formation of a co-repressor complex that inactivates PPAR-γ function through histone H3-K9 methylation. These findings suggest that the non-canonical Wnt signalling pathway suppresses PPAR-γ function through chromatin inactivation triggered by recruitment of a repressing histone methyltransferase, thus leading to an osteoblastic cell lineage from mesenchymal stem cells.

Histone modification on chromatin regulates transcription. Several post-translational and covalent modifications of histones have been documented, for example, methylation of lysine and arginine residues, acetylation of lysine, phosphorylation of serine and threonine residues and sumoylation of lysine. Accumulating evidence has established that hyperacetylation of histone in specific chromosomal regions generally results in activation of a given chromatin area in gene regulation, whereas hypoacetylated histones are indicators of inactive chromatin[1–3]. Other histone modifications are less predictable in how they activate chromatin; however, specific combinations of several histone modifications at certain histone residues are considered to constitute a 'histone code' that defines chromatin states for transcriptional control[1]. Among such histone modifications, lysine methylation results in unique transcriptional outcomes depending on the methylation sites, which act as docking signals for recruiting chromatin remodellers and modifiers[2–4]. Among methylated sites on mammalian chromatin, methylated H3-K9, H3-K27 and H4-K20 are considered as hallmarks of a condensed chromatin state[2]. Furthermore, H3-K9 methylation by histone lysine methyltransferase (HKMTs) triggers heterochromatin formation and transcriptionally silences euchromatic regions by recruiting heterochromatin proteins[3,4]. Reflecting the crucial roles of methylated lysines at specific sites, multiple HKMTs have been identified that recognize the same lysine residue for mono-, di- and/or tri-methylations, although the biological role of each HKMT remains elusive[4,5]. Histone modifications are altered during cell-lineage decisions, and rearrangements of histone modifications take place in response to changes in the extracellular environment[6]. However, the molecular mechanisms underlying these processes remain poorly understood.

Certain nuclear receptors (NRs) have been well researched and have been shown to integrate their ligand signals into the histone code through histone acetylation or deacetylation[7,8]. In the absence of cognate ligands, NRs are transcriptionally silent, associating with

[1]Institute of Molecular and Cellular Biosciences, University of Tokyo, Yayoi 1-1-1, Bunkyo-ku, Tokyo 113-0032, Japan. [2]ERATO, Japan Science and Technology, Honcho 4-1-8, Kawaguchi, Saitama 332-0012, Japan. [3]Department of Medicine and Bioregulatory Sciences, Institute of Health Biosciences, University of Tokushima Graduate School, Kuramoto-3, Tokushima, 770-8503, Japan. [4]Center for Animal Resources and Development (CARD), Graduate School of Medical and Pharmaceutical Sciences, Kumamoto University, Honjo 2-2-1, Kumamoto 860-0811, Japan. [5]Okazaki Institute for Integrative Bioscience, National Institutes of Natural Sciences, Okazaki, Aichi 444-8787, Japan. [6]Department of Genome Sciences, Graduate School of Medicine, Kobe University, Kobe 650-0017, Japan. [7]Department of Molecular Cell Biology, Medical Research Institute and School of Biomedical Science, Tokyo Medical and Dental University, and CREST, JST, Kanda-Surugadai, Chiyoda-ku, Tokyo 101-0062, Japan. [8]Department of Molecular Biology, Graduate School of Science, Nagoya University, Chikusa-ku, Nagoya 464-8602, Japan.
[9]Correspondence should be addressed to S.K. (uskato@mail.ecc.u-tokyo.ac.jp)

Received 20 June 2007; accepted 14 September 2007; published online 21 October 2007; DOI: 10.1038/ncb1647

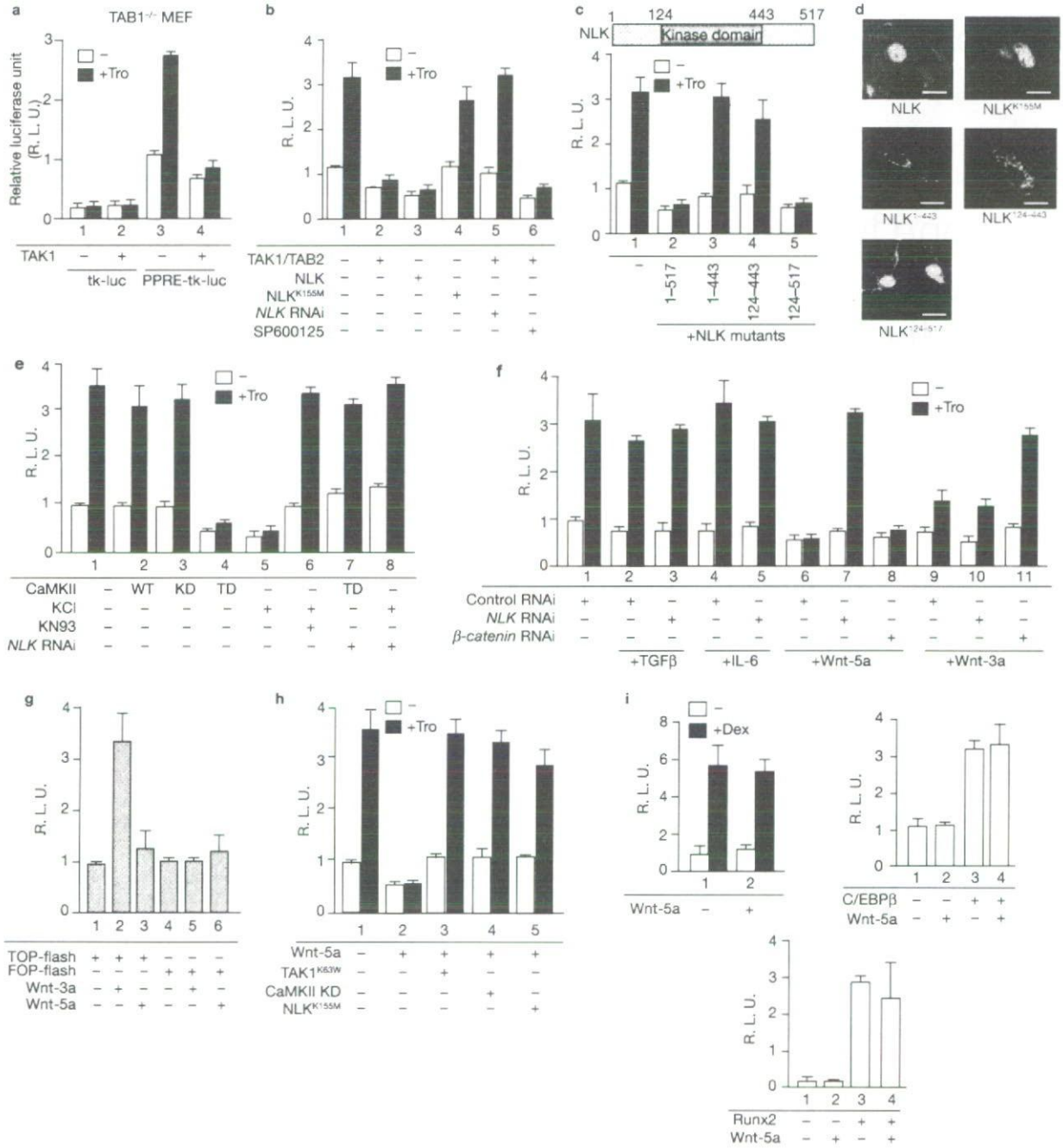

Figure 1 Wnt-5a signalling suppresses the transactivation function of PPAR-γ through CaMKII–TAK1–TAB2–NLK. (**a**) Luciferase assays in TAB1$^{-/-}$ MEF cells. After transfection with PPAR-γ, TAK1 expression vectors and acyl-CoA-PPRE-tk or tk luciferase vectors (tk-luc, thymidine-kinase-promoter–luciferase), cells were incubated with or without troglitazone (Tro). (**b**) Luciferase assays in ST2 cells transfected with PPRE-tk-luc vector and indicated expression vectors (TAK1, TAB2, PPAR-γ, NLK wild-type and kinase-negative mutants NLK^{K155M}), *NLK* RNAi or JNK inhibitor (SP600125). (**c**) Luciferase assays in ST2 cells transfected with PPRE-tk-luc vector and expression vectors of PPAR-γ and NLK deletion mutants. (**d**) ST2 cells transfected with expression vectors of GFP-fusion NLKs were scanned using a Zeiss confocal laser scanning system 510. Scale bars, 50 μm. (**e**) Luciferase assays in ST2 cells transfected with PPRE-tk-luc vector and expression vectors of PPAR-γ, CaMKII or *NLK* RNAi. WT; wild type, TD; active form, KD; kinase-dead form. Luciferase assay in ST2 cells incubated with 50 mM KCl or CaMKII inhibitor (KN93) were also performed (lane 5, 6). (**f**) Luciferase assay in ST2 cells with or without TGF-β, IL-6, Wnt-5a and Wnt-3a. *NLK* or *β-catenin* RNAi was also transfected (lane 3, 5, 7, 8, 10, 11). (**g**) Luciferase assays in ST2 cells transfected with TOP-flash or FOP-flash luc vector (TOP-flash: luc vector containing wild-type β-catenin–TCF-binding site; FOP-flash: luc vector containing mutated β-catenin–TCF-binding site) and incubated with or without Wnt-3a or Wnt-5a. (**h**) Luciferase assays in ST2 cells transfected with PPRE-tk-luc vector and PPRE-γ expression vector with or without Tro, Wnt-5a and indicated expression vectors. (**i**) Luciferase assays in ST2 cells transfected with GR (GR expression vector and GRE-luc), C/EBPβ (C/EBPβ expression vector and C/EBP-RE-tk-luc) or Runx2 (Runx2 expression vector and Runx2-RE-tk-luc). Dexamethasone (100 nM) was used to induce glucocorticoid receptor function. All error bars represent the means±s.d. of triplicate determinations (n=5×10^4 cells).

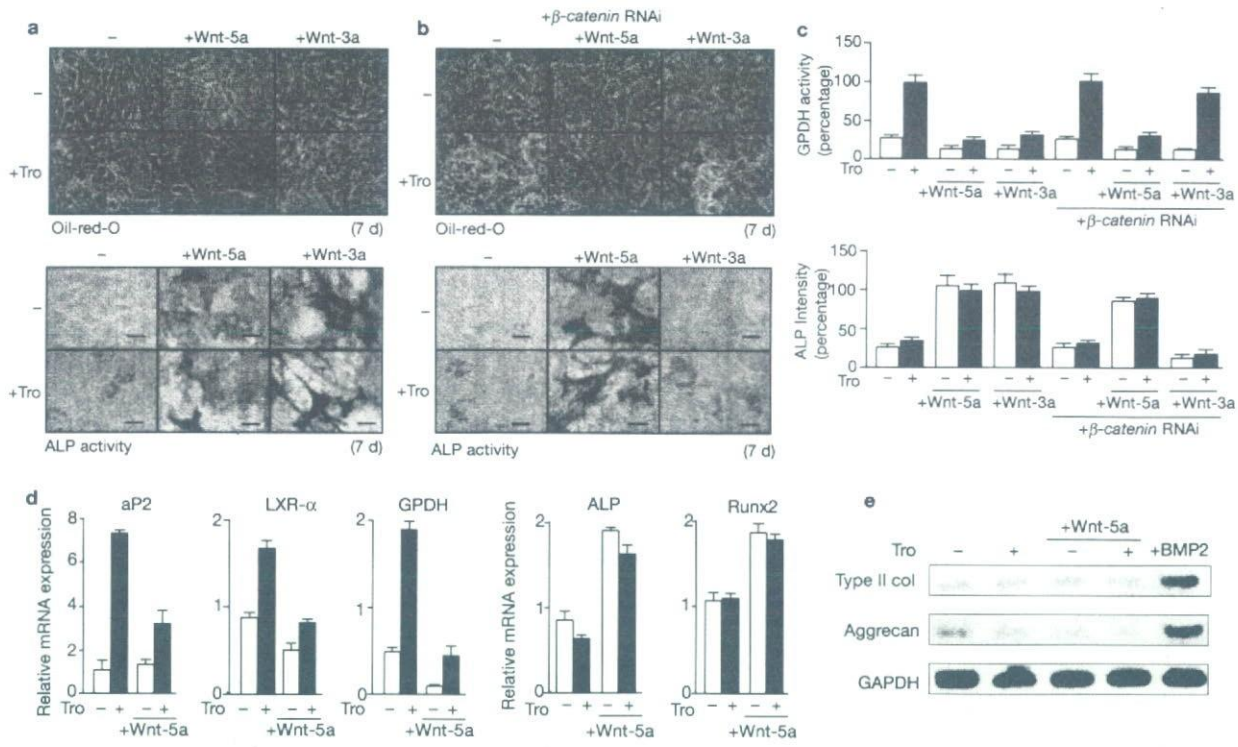

Figure 2 Wnt-5a inhibits adipogenesis and induces osteoblastogenesis in bone marrow mesenchymal stem cells. (**a**) ST2 cells incubated with or without troglitazone (Tro), Wnt-3a or Wnt-5a for 7 days were stained with Oil-Red-O (top) or for alkaline phosphatase (ALP) activity (bottom). (**b**) After transfection with β-*catenin* RNAi, ST2 cells were incubated and stained as in **a**. (**c**) Top, glycerol-3-phosphate dehydrogenase (GPDH) activities were measured using a GPDH assay kit. Bottom, measurement graph of ALP activities (A_{410}) in each cell. Error bars represent the means±s.d. of triplicate determinations. $n=3\times10^6$ cells. (**d**) Quantitative RT–PCR of differentiation markers of adipocyte (aP2, GPDH, LXR-α) and osteoblast (Runx2 and ALP) in ST2 cells treated with/without Tro or Wnt-5a. Error bars represent the means±s.d. of triplicate determinations. $n=3\times10^6$ cells. Expression levels were normalized for GAPDH expression. (**e**) RT–PCR analysis for differentiation markers of chondrocyte (type II collagen and aggrecan) in ST2 cells incubated with or without Wnt-5a, BMP2 and Tro was performed. Scale bars, 100 μm.

co-repressors or co-repressor complexes that often contain histone deacetylases (HDAC), which render histones hypoacetylated. Ligand binding to NRs induces clearance of such HDAC co-repressors, leading to recruitment of a co-activator or co-activator complexes in which histone acetyltransferase (HAT) activity is often detectable[7,8]. Besides ligand-induced transactivation through co-regulator switching, NRs mediate ligand-dependent and -independent transrepression through cross-talk with other intracellular signalling pathways through multiple processes of gene regulation[9].

PPAR-γ is an important NR in many biological events such as cell differentiation and cell-lineage decisions[10–12]. In particular, adipogenesis from pleiotrophic mesenchymal stem cells is primarily induced by PPAR-γ upon agonist binding[13]. However, such PPAR-γ function in adipogenesis seems to be modulated through cross-talk with other cellular signalling pathways[14]. For instance, even though bone mesenchymal stem cells are primed by PPAR-γ agonists for adipogenesis, suppression of PPAR-γ function by cytokines in progenitor cells converts the cell fate of adipogenic precursors into osteoblastic cells[15]. Osteoblastogenesis is governed by a number of regulators including Wnt peptide ligands[16–18]. Canonical and non-canonical Wnt signalling pathways are activated by multiple Wnt ligands through binding to frizzled (Fzd) plasma-membrane receptors. During activation of the canonical pathway, stabilization and nuclear translocation of the intracellular transducer β-catenin induces it to associate with members of the TCF-LEF (T-cell factor lymphoid enhancer factor) family of transcriptional factors for transcriptional activation[19]. However, downstream cascades from the non-canonical signal[20,21] remain to be uncovered and their role in mesenchymal stem-cell differentiation remains obscure.

Osteoblastogenesis is dominant over adipogenesis in the bone marrow of young animals and the cell-differentiation balance between the two cell types is usually reversed in bone marrow of elder or osteoporotic animals[18]. Therefore, we reasoned that PPAR-γ function is suppressed in the bone marrow of young animals. In the present study, we reveal that transactivation of agonist-bound PPAR-γ is repressed by a non-canonical cascade activated by Wnt-5a through the phosphorylated H3-K9 HMKT, SETDB1 (refs 22, 23) in a complex with NLK (ref. 20) and CHD7 (chromodomain helicase DNA-binding protein 7; ref. 24). This leads to a change of cell fate from adipogenesis to osteoblastogenesis of bone marrow mesenchymal stem cells even in the presence of a PPAR-γ agonist. Thus, these findings reveal a new molecular mechanism where a signal from a cell membrane receptor leads to altered histone modification and changes in gene regulation and cell-lineage decisions.

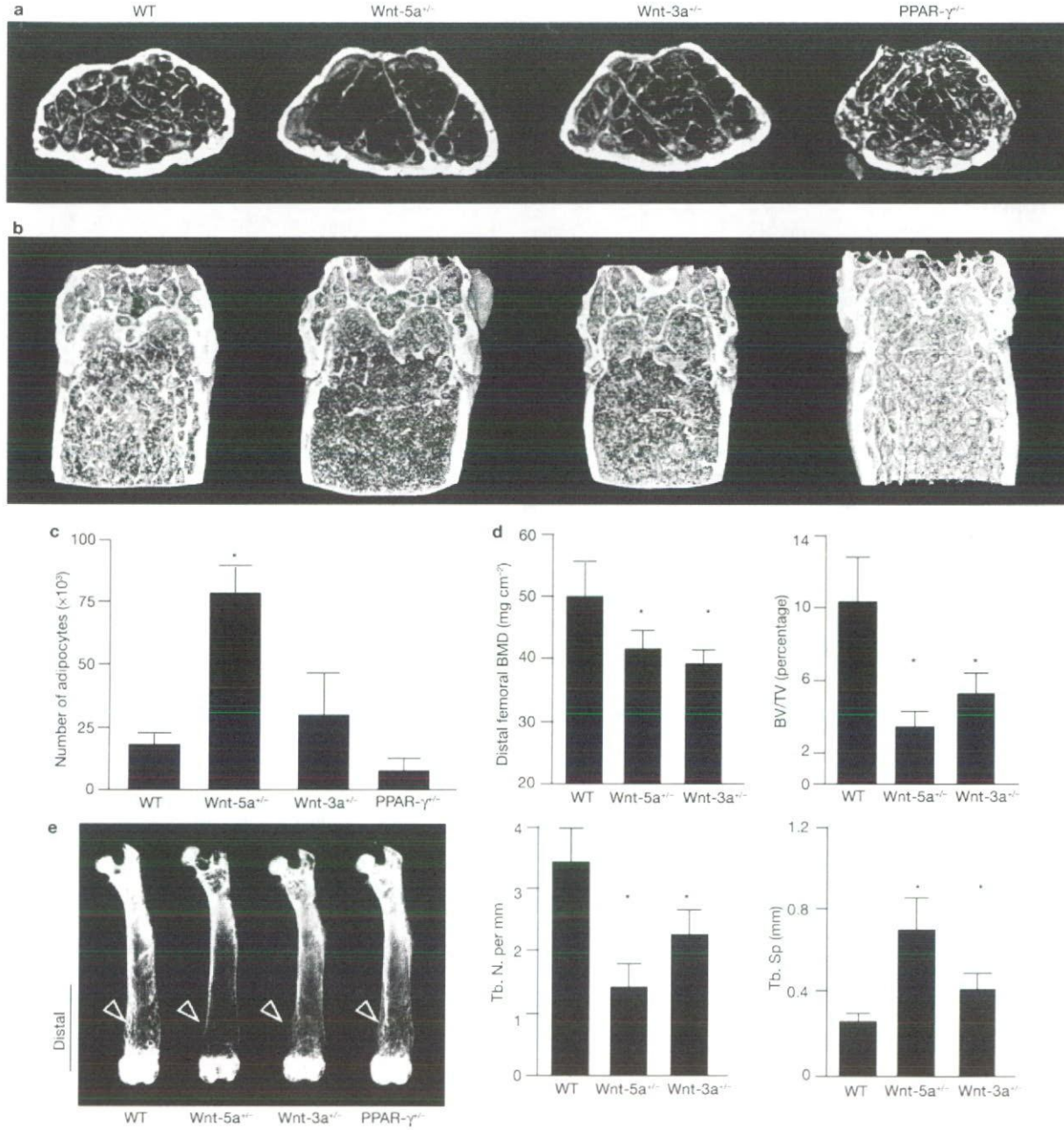

Figure 3 Bone analysis of distal femora of 18-weeks-old WT, Wnt-5a$^{+/-}$, Wnt-3a$^{+/-}$ and PPAR-γ$^{+/-}$ male mice. (**a**, **b**) Three-dimensional computational tomography images of distal femora of representative WT, Wnt-5a$^{+/-}$, Wnt-3a$^{+/-}$ and PPAR-γ$^{+/-}$ mice. In (**b**), adipocytes are displayed as orange. (**c**) The number of adipocytes was histologically measured. (**d**) Bone mineral density (BMD) of distal femora, trabecular bone volume per tissue volume (BV/TV), trabecular number (Tb. N.) and trabecular space (Tb. Sp.) were measured on the CT image. In (**c**) and (**d**), bars indicate means±s.d.(n=5 to 7 animals per genotype); Student's t-test; *, P<0.05 versus WT. (**e**) Soft x-ray image of femora from 18-week-old WT, Wnt-5a$^{+/-}$, Wnt-3a$^{+/-}$ and PPAR-γ$^{+/-}$ male mice.

RESULTS

NLK represses the transactivation function of PPAR-γ through a CaMKII–TAK1–TAB2 cascade

We previously reported that activated NF-κB transcriptionally represses activated PPAR-γ through a TAB1–TAK1-mediated (TAB1, TAK1-binding protein 1; TAK1, TGFβ-activated protein kinase 1) cascade activated by cytokines[15]. However, using TAB1$^{-/-}$ mouse embryonic fibroblast (MEF) cells[25], we unexpectedly found that TAK1 was still able to repress activated PPAR-γ in the presence of a synthetic agonist, troglitazone (Tro) (Fig. 1a). Because TAK1 serves as a mediator for other signalling cascades[20,26], we searched for a partner for TAK1 and found TAB2. By searching for downstream factors using a transient expression assay in ST2 cells (bone-marrow-derived stromal cells), a mitogen-activated protein (MAP)-kinase-like kinase, NLK, was found to replace TAK1–TAB2 and repress activated PPAR-γ (Fig. 1b). The wild-type (WT) and deletion mutants of NLK, which were potent repressors of PPAR-γ were

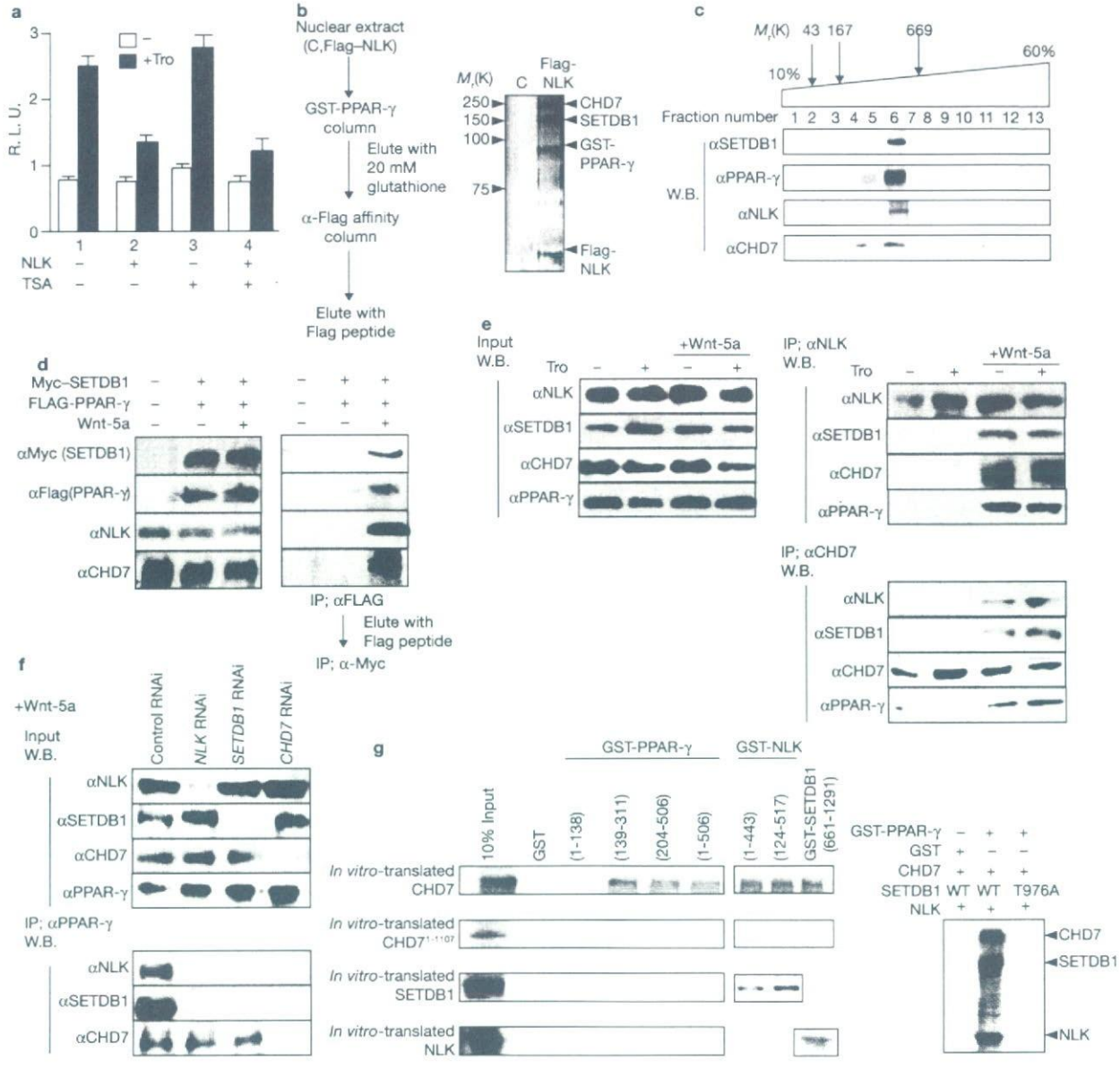

Figure 4 SETDB1 and CHD7 form a complex with PPAR-γ and NLK in a Wnt-5a-dependent manner. (**a**) Luciferase assays in ST2 cells treated with or without HDAC inhibitor (1 μM TSA) after transfection with PPAR-γ and NLK expression vectors and PPRE-tk-luc vector. Error bars represent the mean±s.d. of triplicate determinations. (**b**) Purification of the PPAR-γ–NLK complex from Flag–NLK-expressing HeLa cells using GST–PPAR-γ affinity column followed by anti-Flag immunocolumn chromatography. (**c**) Analysis of NLK–PPAR-γ complex by glycerol density gradient followed by western blotting with anti-SETDB1 and anti-CHD7 antibodies. (**d**) Two-step immunoprecipitation. ST2 cells were transfected with Flag–PPAR-γ and Myc–SETDB1 and then treated with Tro and/or Wnt-5a. Nuclear extracts were immunoprecipitated with anti-Flag and eluted with the Flag peptide. Then anti-Flag immunocomplexes were immunoprecipitated with anti-Myc and probed by western blotting with indicated antibodies. (**e**) Immunoprecipitation assay in ST2 cells after treatment with or without Tro and Wnt-5a. Nuclear extracts were immunoprecipitated with anti-NLK and anti-CHD7 antibodies. Immunoprecipitants were detected by western blotting with indicated antibodies. Uncropped images of the blots are shown in the Supplementary Information, Fig. S6a. (**f**) Immunoprecipitation assay from cells RNAi-knockdown NLK, SETDB1 or CHD7. After infection with Adeno X-RNAi against NLK, SETDB1 and CHD7 in ST2 cells, cells treated with Wnt-5a were lysed and immunoprecipitated with anti-PPAR-γ antibody. Immunocomplexes were analysed by western blotting with indicated antibodies. (**g**) GST fusion proteins of NLK, PPAR-γ and SETDB1 were expressed in *E. coli* and used in GST pull-down assays with [^{35}S]-methionine-labelled CHD7 or CHD7$^{1-1107}$. Compared with CHD7, CHD7$^{1-1107}$ did not bind to PPAR-γ, NLK and SETDB1. When [^{35}S]-methionine-labelled CHD7, SETDB1 and NLK were incubated with GST-PPAR-γ, all components were associated with GST-PPAR-γ (right panel).

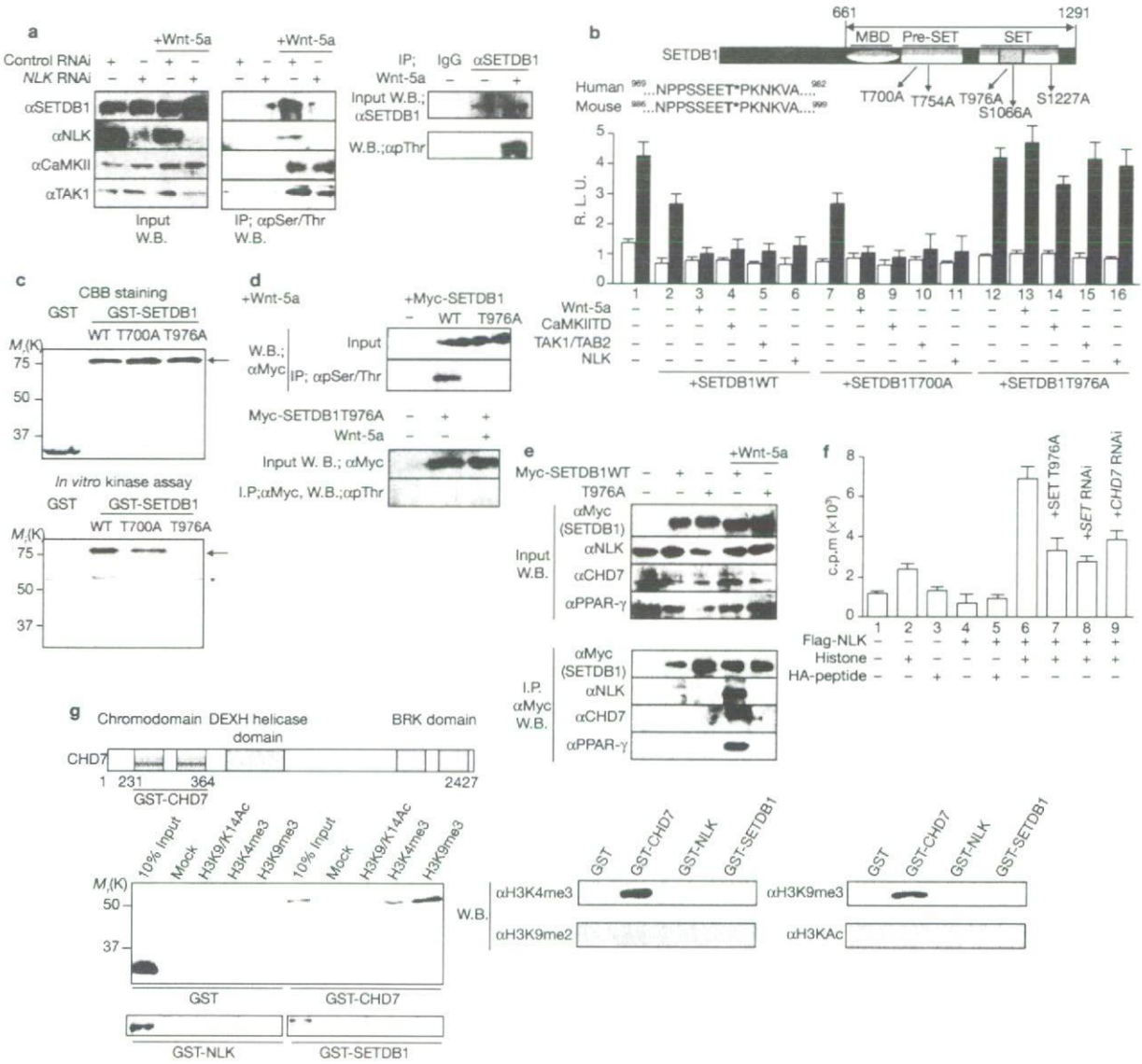

Figure 5 Phosphorylated SETDB1 forms a complex with CHD7–NLK–PPAR-γ. (**a**) Left and middle panel, lysates of ST2 cells treated with or without Wnt-5a and transfected with control or *NLK* RNAi were applied to anti-Ser–Thr phosphorylation columns, then probed with indicated antibodies. Uncropped images of the blots are shown in the Supplementary Information, Fig. S6b. Right panel, lysates of ST2 cells treated with or without Wnt-5a were immunoprecipitated by IgG or anti-SETDB1 and then probed by anti-phosphothreonine (pThr). (**b**) Predicted phosphorylation sites of SETDB1 (661–1291). Thr976 is conserved between humans and mice. Luciferase assays in ST2 cells transfected with PPRE-tk-luc vector, PPAR-γ expression vector and indicated expression vectors were performed. Error bars represent the mean±s.d. of triplicate determinations. n=5×10⁴ cells. (**c**) NLK phosphorylates GST–SETDB1 *in vitro*. Upper panels, GST-fusion SETDB1 (WT, T976A and T700A) proteins were stained with CBB (upper panel, arrow indicates GST–SETDB1). Lower panels, the *in vitro* kinase assay was performed as described in the methods. (Arrow indicates GST–SETDB1, and the asterisk indicates self-phosphorylated NLK.) (**d**) SETDB1 T976A is not phosphorylated *in vivo*. Upper panel, after transfection with the indicated expression vector, immunoprecipitation with anti-Ser–Thr phosphorylation columns and western blotting was performed. Lower panel, after transfection with Myc–SETDB1T976A expression vector, cell extracts were immunoprecipitated with anti-Myc and probed with anti-phosphothreonine. (**e**) Immunoprecipitation assay in ST2 cells. After transfection with Myc–SETDB1 or SETDB1 T976A expression vector, immunoprecipitation with anti-Myc sepharose and western blotting were performed using the indicated antibodies. (**f**) NLK immunocomplexes possess histone methyltransferase activity. After transfection with Flag–NLK expression vector and the indicated vector and RNAi, in ST2 cells and immunoprecipitation with anti-Flag column, HMT assays were performed. Error bars represent the means±s.d. of triplicate determinations. n=5×10⁴ cells. (**g**) Upper panel, the peptide pull-down assay was performed using purified GST and GST-fused proteins with various modified H3 peptides (1–21 a.a.) indicated on top. Bound proteins were analysed by SDS-PAGE and silver staining. Lower panels, histone-binding assays were performed using HeLa histone extract and GST, GST–CHD7, –NLK and –SETDB1. Bound proteins were analysed by SDS-PAGE and western blotting. Uncropped images of the blots are shown in Supplementary Information, Fig. S6c.